Table 1 Characteristics of giant coronary artery aneurysms with a diameter more than 50 mm without fistula

Author	Max diameter (mm)	Sex	Age (years old)	Coronary	Cause	Symptom	Treatment
Kumar G [9]	160	F	73	RCA	Fibromuscular dysplasia	SVC syndrome	Surgery (died)
Kim SH [10]	150	F	61	RCA	Atherosclerotic	SOB	Surgery
Zhang CC [11]	150	F	25	RCA	Congenital	Palpitation, SOB	Surgery
Lim CH [12]	150	M	34	RCA	Congenital	SOB	Surgery
Wei J [13]	150	F	26	RCA	Congenital	Cough, SOB	Surgery
Chazov E [14]	120	M	45	RCA	Unknown	Chest heaviness, dyspnea	Surgery
Westaby S [15]	120	M	70	RCA	Unknown (Atherosclerotic?)	Chest pain	Surgery
Westaby S [15]	110	M	71	RCA	Unknown (Atherosclerotic?)	Chest pain, collapse	Surgery
Konen E [16]	101	M	54	RCA	Unknown	Fatigue	Surgery
Jönsson A [17]	100	F	55	LMT	Atherosclerotic	Fatigue, dyspnea	Surgery
Tanabe M [18]	96	M	53	LCX	NA	No	Surgery
McGlinchey PG [19]	96	F	45	RCA	NA	Sensation of fullness in chest, palpitation, edema	Surgery
Kobayashi T [20]	86	NA	18	RCA	Kawasaki disease	No	Surgery
Channon KM [21]	85	M	72	RCA	Atherosclerotic	No	Surgery
LaMendola CL [22]	80	M	75	RCA	Atherosclerotic?(systemic)	No	Surgery
Bauer M [23]	80	F	46	RCA	Atherosclerotic	Thoracic discomfort, dyapnea	Surgery
Selke KG [24]	80	F	30	RCA	Congenital	Chest pain	Surgery
Strouse D [7]	80	M	79	RCA	Atherosclerotic	No	Surgery
Grandmougin D [25]	75	NA	46	RCA	Atherosclerotic	CHF, OMI	Surgery
Collons MJ [26]	75	M	45	RCA	Atherosclerotic	Arrhythmia, MVP	Surgery
Kwon T-G [27]	75	F	68	LAD	NA	Collapse	Surgery
Perteson MA [28]	>70	M	61	RCA, LCX	Unknown	Dyspnea on exertion	Surgery, PCI
Anania A [29]	70	M	71	LAD	Atherosclerotic?	No	Medical
Hirsch GM [30]	70	M	71	RCA	Medial fibromuscular dysplasia and atherosclerosis	No	Surgery
Augustin N [31]	62	F	31	RCA	Vasculitis	Syncope, dyspnea on exertion	Surgery
Suzuki H [32]	60	F	71	LMT	Takayasu aortitis	Sudden death	Medical (died)
Channon KM [33]	60	M	72	RCA	Atherosclerotic	Chest pain	Surgery
Banerjee P [34]	53	F	69	RCA	Kawasaki disease?	Chest pain (AMI)	Medical (warfarin)
Luckraz H [35]	>50	M	68	LAD	Atherosclerotic	Chest pain, SOB	Surgery
Ebina T	50	M	40	LAD	Kawasaki disease?	No	Surgery
Nobrega TP [36]	50	F	26	RCA	SLE	No	Medical
Wolford DC [37]	50	M	80	LCX	Atherosclerotic?	Chest pain	Surgery
Staumann E [38]	50	M	43	RCA	Congenital?	Chest pain	Surgery
Kanemitsu N [39]	50	F	74	SNA	Atherosclerotic	Chest pain	Surgery

RCA, right coronary artery; LMT, left main trunk; LAD, left anterior descending artery; LCX, left circumflex artery; SNA, sinus node artery; SVC, superior vena cava; SLE, systemic lupus erythematosus; SOB, shortness of breath; CHF, congestive heart failure; OMI, old myocardial infarction; MVP, mitral valve prolapse; PCI, percutaneous coronary intervention; AMI, acute myocardial infarction; NA, not available.

artery is the RCA. Symptoms are chest pain, dyspnea, palpitation, and so on. However, sometimes it is asymptomatic as shown in this case. Resection of coronary artery aneurysm with CABG is most frequently performed as the treatment of giant coronary artery aneurysms.

Conclusion

We reported a case with giant coronary artery aneurysm with the diameter of 50 mm probably due to Kawasaki disease, and reviewed the literature on giant coronary artery aneurysms.

References

[1] Wright WP, Alpert MA, Mukerji V, Santolin CJ. Coronary artery aneurysm—a case study and literature review. Angiology 1991;42:672—9.

[2] Kawasaki T. Acute febrile mucocutaneous syndrome with lymphoid involvement with specific desquamation of the fingers and toes in children. Jpn J Allergy 1967;16:178—222 [in Japanese].

[3] Dajani AS, Taubert KA, Gerber MA, Shulman ST, Ferrieri P, Freed M, et al. Diagnosis and therapy of Kawasaki disease in children. Circulation 1993;87:1776—80.

[4] Gersony WM. Diagnosis and management of Kawasaki disease. JAMA 1991;265:2699—703.

[5] Burns JC, Shike H, Gordon JB, Malhotra A, Schoenwetter M, Kawasaki T. Sequelae of Kawasaki disease in adolescents and young adults. J Am Coll Cardiol 1996;28:253—7.

[6] Tunick PA, Slater J, Kronzon I, Glassman E. Discrete atherosclerotic coronary artery aneurysms: a study of 20 patients. J Am Coll Cardiol 1990;15:279—82.

[7] Strouse D, Katz ES, Tunick PA, Winer HE, Krinsky GA, Galloway AC, et al. Diagnosis of a giant coronary aneurysm with multiple imaging modalities. Echocardiography 2000;17:173—6.

[8] Mawatari T, Koshino T, Morishita K, Komatsu K, Abe T. Successful surgical treatment of giant coronary artery aneurysm with fistula. Ann Thorac Surg 2000;70:1394—7.

[9] Kumar G, Karon BL, Edwards WD, Puga FJ, Klartich KW. Giant coronary aneurysm causing superior vena cava syndrome and congestive heart failure. Am J Cardiol 2006;98:986—8.

[10] Kim SH, Jang IS, Ouck CCD, Kim CW, Choi JY, Kim HJ, et al. Giant atherosclerotic aneurysm of the sinoatrial nodal artery. J Thorac Cardiovasc Surg 1997;114:280—2.

[11] Zhang CC, Hu LX, Hsieh SW, Liu JF. Echocardiographic features of a giant congenital aneurysm of the right coronary artery. J Clin Ultrasound 1988;16:502—5.

[12] Lim CH, Tan NC, Tan L, Seah CS, Tan D. Giant congenital aneurysm of the right coronary artery. Am J Cardiol 1977;39:751—3.

[13] Wei J, Wang DJ. A giant congenital aneurysm of the right coronary artery. Ann Thorac Surg 1986;41:322—4.

[14] Chazov E, Akchurin R, Lepilin M, Agapov A, Belyaev A, Partigulov S, et al. Giant aneurysm of the coronary artery. Int Angiol 1991;10:106—11.

[15] Westaby S, Vaccari G, Katsumata T. Direct repair of giant coronary aneurysm. Ann Thorac Surg 1999;68:1401—3.

[16] Konen E, Feinberg MS, Morag B, Guetta V, Shinfeld A, Smolinsky A, et al. Giant right coronary aneurysm: CT angiographic and echocardiographic findings. Am J Roentgenol 2001;177:689—91.

[17] Jönsson A, Nilsson T, Pernow J, Ivert T. Resection of a giant left main stem coronary artery aneurysm. J Cardiovasc Surg 2001;42:489—91.

[18] Tanabe M, Onishi K, Hiraoka N, Kitamura T, Okinaka T, Ito M, et al. Bilateral giant coronary aneurysms diagnosed noninvasively by dynamic magnetic resonance imaging. Int J Cardiol 2004;94:341—2.

[19] McGlinchey PG, Maynard SJ, Graham AN, Roberts MJD, Khan MM. Giant aneurysm of the right coronary artery compressing the right heart. Circulation 2005;112:e66—7.

[20] Kobayashi T, Sone K, Shinohara M, Kosuda T, Kobayashi T. Giant coronary aneurysm of Kawasaki disease developing during postacute phase. Circulation 1998;98:92—3.

[21] Channon KM, Wadsworth S, Bashir Y. Giant coronary artery aneurysm presenting as a mediastinal mass. Am J Cardiol 1998;82:1307—8.

[22] LaMendola CL, Culliford AT, Harris LJ, Amendo MT. Multiple aneurysms of the coronary arteries in a patient with systemic aneurysmal disease. Ann Thorac Surg 1990;49:1009—10.

[23] Bauer M, Redzepagic S, Weng Y, Hetzer R. Successful surgical treatment of a giant aneurysm of the right coronary artery. Thorac Cardiovasc Surgeon 1998;46:152—4.

[24] Selke KG, Vemulapalli P, Brodarick SA, Coordes C, Gowda S, Salem B, et al. Giant coronary artery aneurysm: detection with echocardiography, computed tomography, and magnetic resonance imaging. Am Heart J 1991;121:1544—7.

[25] Grandmougin D, Croisille P, Robin C, Péoc'h M, Barral X. Giant coronary artery aneurysm mimicking a compressive cardiac tumor. Imaging features and operative strategy. Cardiovasc Pathol 2005;14:272—5.

[26] Collins MJ, Borges AJ, Singh G, Pillai JB, David TE, Leong SW, et al. A giant coronary artery aneurysm in the right coronary artery. Cardiovasc Pathol 2006;15:150—2.

[27] Kwon T-G, Yoon D-W, Hyun D-W, Kim K-Y, Bae J-H. A giant coronary artery aneurysm presenting with cardiac tamponade. Int J Cardiol 2007;119:e46—7.

[28] Peterson MA, Monsein LH, Dangas G, Mehran R, Leon MB. Percutaneous transcatheter management of giant coronary aneurysms. Circulation 1999;100:e8—11.

[29] Anania A, Trapani M, Striglia E, Sambuco A, Longato L, Tarocco RP. Giant coronary artery aneurysm in association with systemic arterial ectasia. A case report. Minerva Cardioangiol 2006;54:169—72.

[30] Hirsch GM, Casey PJ, Raza-Ahmad A, Miller RM, Hirsch KJ. Thrombosed giant coronary artery aneurysm presenting as an intracardiac mass. Ann Thorac Surg 2000;69:611—3.

[31] Augustin N, Wessely R, Pörner M, Schömig A, Lange R. Giant coronary aneurysm obstructing the right heart. Lancet 2006;368:386.

[32] Suzuki H, Daida H, Tanaka M, Sato H, Kawai S, Sakurai H, et al. Giant aneurysm of the left main coronary artery in Takayasu aortitis. Heart 1999;81:214—7.

[33] Channon KM, Banning AP, Davies CH, Bashir Y. Coronary artery aneurysm rupture mimicking dissection of the thoracic aorta. Int J Cardiol 1998;65:115—7.

[34] Banerjee P, Houghton T, Walters M, Kaye GC. Giant right coronary artery aneurysm presenting as a mediastinal mass. Heart 2004;90:e50—1.

[35] Luckraz H, Parums DV, Dunning J. Reverse saphenous interposition vein graft repair of a giant atherosclerotic aneurysm of the left anterior descending coronary artery. J Thorac Cardiovasc Surg 2002;123:817—20.

[36] Nobrega TP, Klodas E, Breen JF, Liggett SP, Higano ST, Reeder GS. Giant coronary artery aneurysms and myocardial infarction in a patient with systemic lupus erythematosus. Cathet Cardiovasc Diagn 1996;39:75–9.
[37] Wolford DC, Jost CMT, Madu EC, Walker W, Ramanathan KB. Role of transesophageal echocardiography in the clinical management of a patient with a giant coronary artery aneurysm. Clin Cardiol 1997;20:573–5.
[38] Straumann E, Niederhäuser U, Meili C, Christen S, Bertel O. Recurrent myocardial infarction caused by a giant coronary aneurysm. Int J Cardiol 1998;63:305–7.
[39] Kanemitsu N, Nakamura T, Okabe M, Tenpaku H, Wariishi S, Ohki A. Giant coronary artery aneurysm from sinus node artery. Ann Thorac Surg 2001;72:1373–4.

Sarcalumenin is essential for maintaining cardiac function during endurance exercise training

Qibin Jiao, Yunzhe Bai, Toru Akaike, Hiroshi Takeshima, Yoshihiro Ishikawa and Susumu Minamisawa

Am J Physiol Heart Circ Physiol 297:H576-H582, 2009. First published 5 June 2009;
doi:10.1152/ajpheart.00946.2008

AJP - Heart and Circulatory Physiology publishes original investigations on the physiology of the heart, blood vessels, and lymphatics, including experimental and theoretical studies of cardiovascular function at all levels of organization ranging from the intact animal to the cellular, subcellular, and molecular levels. It is published 12 times a year (monthly) by the American Physiological Society, 9650 Rockville Pike, Bethesda MD 20814-3991. ISSN: 0363-6135, ESSN: 1522-1539. Visit our website at http://www.the-aps.org/.

Am J Physiol Heart Circ Physiol 297: H576–H582, 2009.
First published June 5, 2009; doi:10.1152/ajpheart.00946.2008.

Sarcalumenin is essential for maintaining cardiac function during endurance exercise training

Qibin Jiao,[1] Yunzhe Bai,[1] Toru Akaike,[1] Hiroshi Takeshima,[2] Yoshihiro Ishikawa,[1,3] and Susumu Minamisawa[1,4,5]

[1]*Cardiovascular Research Institute, Yokohama City University Graduate School of Medicine, Yokohama, Japan;* [2]*Department of Medical Chemistry, Kyoto University Graduate School of Pharmaceutical Science, Kyoto, Japan;* [3]*Cardiovascular Research Institute, Departments of Cell Biology and Molecular Medicine and Medicine (Cardiology), New Jersey Medical School, Newark, New Jersey;* [4]*Department of Life Science and Medical Bioscience, and* [5]*Institute for Biomedical Engineering, Consolidated Research Institute for Advanced Science and Medical Care, Waseda University, Tokyo, Japan*

Submitted 22 August 2008; accepted in final form 2 June 2009

Jiao Q, Bai Y, Akaike T, Takeshima H, Ishikawa Y, Minamisawa S. Sarcalumenin is essential for maintaining cardiac function during endurance exercise training. *Am J Physiol Heart Circ Physiol* 297: H576–H582, 2009. First published June 5, 2009; doi:10.1152/ajpheart.00946.2008.—Sarcalumenin (SAR), a Ca^{2+}-binding protein located in the longitudinal sarcoplasmic reticulum (SR), regulates Ca^{2+} reuptake into the SR by interacting with cardiac sarco(endo)plasmic reticulum Ca^{2+}-ATPase 2a (SERCA2a). We have previously demonstrated that SAR deficiency induced progressive heart failure in response to pressure overload, despite mild cardiac dysfunction in sham-operated SAR knockout (SARKO) mice (26). Since responses to physiological stresses often differ from those to pathological stresses, we examined the effects of endurance exercise on cardiac function in SARKO mice. Wild-type (WT) and SARKO mice were subjected to endurance treadmill exercise training (~65% of maximal exercise ability for 60 min/day) for 12 wk. After exercise training, maximal exercise ability was significantly increased by 5% in WT mice ($n = 6$), whereas it was significantly decreased by 37% in SARKO mice ($n = 5$). Cardiac function assessed by echocardiographic examination was significantly decreased in accordance with upregulation of biomarkers of cardiac stress in SARKO mice after training. After training, expression levels of SERCA2a protein were significantly downregulated by 30% in SARKO hearts, whereas they were significantly upregulated by 59% in WT hearts. Consequently, SERCA2 activity was significantly decreased in SARKO hearts after training. Furthermore, the expression levels of other Ca^{2+}-handling proteins, including phospholamban, ryanodine receptor 2, calsequestrin 2, and sodium/calcium exchanger 1, were significantly decreased in SARKO hearts after training. These results indicate that SAR plays a critical role in maintaining cardiac function under physiological stresses, such as endurance exercise, by regulating Ca^{2+} transport activity into the SR. SAR may be a primary target for exercise-related adaptation of the Ca^{2+} storage system in the SR to preserve cardiac function.

treadmill; calcium uptake; heart failure; excitation-contraction coupling

ENDURANCE EXERCISE IS ONE of the most common physiological stresses affecting the homeostasis of the whole body. Adaptations to chronic endurance exercise result in functional and structural changes in the heart (19, 31, 33); for example, after chronic endurance exercise training, it has been shown that resting heart rate is decreased and that maximal stroke volume is increased, since myocardial contractile function is enhanced and left-ventricular cavity dimension is augmented (2, 14, 25). A growing body of evidence has demonstrated that the regulation of intracellular Ca^{2+} through the sarcoplasmic reticulum (SR) plays a critical role in maintaining cardiac function under both physiological and pathological stresses (5, 7, 17). In particular, rapid transport of Ca^{2+} from the cytosol to the SR via the cardiac sarco(endo)plasmic reticulum Ca^{2+}-ATPase 2a (SERCA2a) is a critical determinant for the maintenance of Ca^{2+} storage in the SR. Therefore, it is extremely important for us to understand the effect of endurance exercise training on SERCA2a function and thus on the Ca^{2+} storage system in the heart. In this regard, a considerable number of previous studies on animals have demonstrated that endurance exercise training increases the expression and/or activity of SERCA2a in the heart, resulting in enhanced cardiac function of the healthy (9, 10, 20, 22, 30, 35) or pathological heart (6, 15, 21, 24, 34, 39).

Sarcalumenin (SAR) is an SR luminal glycoprotein responsible for Ca^{2+} buffering in skeletal and cardiac muscles (13, 16). SAR is predominantly found in the longitudinal SR, where SERCA and phospholamban (PLN) are also located. Our laboratory's previous study has demonstrated that SAR interacts with SERCA2 to enhance the protein stability of SERCA2a, and that it facilitates Ca^{2+} sequestration into the cardiac SR (26). Although young sedentary SAR knockout (SARKO) mice exhibit only mild impairments in Ca^{2+} transient and cardiac function (38), we have recently demonstrated that SAR deficiency induced progressive heart failure in response to pressure overload (26), indicating that SAR plays a critical role in adapting to pathological stresses, such as pressure overload in the heart. We found that SAR is essential for maintaining SERCA2a expression and activity in the pressure-overloaded heart. However, it has recently been reported that skeletal muscle from SARKO mice is highly resistant to fatigue compared with that from wild-type (WT) mice (40); this fatigue resistance of SARKO skeletal muscle is likely due to enhanced store-operated Ca^{2+} entry (SOCE) induced by upregulated expression of mitsugumin 29 (MG29), a synaptophysin-related membrane protein that is not expressed in the heart. In addition, it is known that the heart often responds differently to physiological stresses, such as endurance exercise, than to pathological stresses, such as pressure overload. Therefore, it remains unknown whether SAR also plays a role in maintaining cardiac function when the heart is exposed to physiological stresses, such as endurance exercise. To clarify the mode of action of SAR in the heart under a physiological stress, such as endurance exercise training, we investigated the

Address for reprint requests and other correspondence: S. Minamisawa, Dept. of Life Science and Medical Bioscience, Waseda Univ., 2-2 Wakamatsu-cho, Shinjuku-ku, Tokyo 162-8480, Japan (E-mail: sminamis@waseda.jp).

impact of SAR deficiency on the expression and activity of SERCA2a in the heart and on cardiac function after endurance exercise training.

MATERIALS AND METHODS

Animal preparation. Generation of SARKO mice has been described previously (38). SARKO and C57BL/6J WT mice (8–10 wk of age) were bred at Yokohama City University. All mice used in the present study came from the same genetic background. All animal care and study protocols were approved by the Animal Ethics Committees of Yokohama City University School of Medicine and Waseda University, and the investigation conforms to the Guide for the Care and Use of Laboratory Animals published by the US National Institutes of Health (National Institutes of Health Publication No. 85–23, revised 1996).

Maximal exercise ability and treadmill endurance exercise training. Mice were randomized into four groups: sedentary WT (SED-WT) and sedentary SARKO (SED-SARKO) mice, and WT (ET-WT) and SARKO (ET-SARKO) mice subjected to endurance exercise training.

Animals ran on a rodent motor-driven treadmill (MANUAL, LE 8700 series, Panlab, Barcelona, Spain) with adjustable belt speed (0–150 cm/s). The treadmill apparatus was equipped with adjustable-amperage (0–2 mA) shock bars at the rear of the belt, through which mild electrical stimulation (grid shock <1 mA) was applied to encourage the mice to run. A detector located above the shock grid measured the number of shock stimuli received by each mouse.

First, mice were acclimated to the treadmill via three 15-min running sessions with mild shock stimulation and a belt speed of 30 cm/s. After acclimation, all mice underwent a treadmill exercise test to determine their exercise ability before the endurance exercise training described below; a similar assessment was made during and after training for comparison purposes. The belt speed of the treadmill was set to 30 cm/s at the beginning of each test. It was then increased linearly by 2 cm/s every 30 s until the mice could not continue to run regularly on the treadmill, or until they had rested on the shock grid more than three times. The final belt speed achieved by each mouse was considered to be that mouse's maximal exercise ability. Maximal exercise ability was determined by averaging the maximal belt speeds of at least three measurements for each mouse; there was an intermission of at least 1 h between each measurement. Workloads of endurance exercise training were then adjusted for each mouse in accordance with its maximal exercise ability.

Before the start of each exercise training session, each mouse performed a 5-min warm-up at 40% of its maximal speed. ET-WT and ET-SARKO mice then ran on the treadmill (at 0° inclination) at 65% of their maximal speeds for 60 min/day, 5 days/wk, for 12 wk. Each mouse's maximal exercise ability was reevaluated every 4 wk, and each mouse's workload was adjusted again based on its current maximal speed (Supplemental Fig. 1). (The online version of this article contains supplemental data.) For sedentary mice, running skill was maintained by treadmill running for 15 min at 0° inclination at a belt speed of 30 cm/s, 3 days/wk.

Citrate synthase activity. As a marker for endurance training, the myocardial citrate synthase (CS) activity was measured at 37°C in the presence of 0.2% Triton X-100 with 20 μg protein sample, as previously described (27, 32). CS activity was also measured in soleus muscle homogenates to assess the efficacy of endurance exercise training.

Cardiac function assessed by echocardiography. Mice were anesthetized with an intraperitoneal injection of Avertin (250 μg/g) and subjected to echocardiography, as described in our laboratory's previous publications (28, 38). Since we have observed that the heart rates of mice decrease after intraperitoneal injection of Avertin, reaching stable minimal levels around 15–20 min after injection (Supplemental Fig. 2), we obtained the echocardiographic data around 15–20 min after injection of Avertin. After the final assessment of cardiac function after endurance training, heart and skeletal (soleus) muscles were immediately placed in chilled phosphate-buffered saline to remove all residual blood. Hearts were then weighed, and left ventricles were immediately frozen in liquid nitrogen and stored at −80°C.

Quantitative RT-PCR analysis. Total RNA was isolated from various tissues using TRIzol reagent (Invitrogen, Carlsbad, CA), as recommended by the manufacturer. Generation of cDNA and RT-PCR analysis was performed as described previously (36, 37). The primers for PCR amplification were designed based on the mouse nucleotide sequences of atrial natriuretic factor (ANF) and brain natriuretic peptide (BNP). The mRNA levels of interest were normalized to mouse glyceraldehyde-3-phosphate dehydrogenase.

Immunoblot analysis. We prepared protein samples from the left ventricular tissues of the sedentary and trained mice, which had been immediately frozen and stored at −80°C after death of the animals. Immunoblot analyses were performed as described previously (26, 36). Briefly, tissues were defrosted to 0°C and homogenized in a chilled homogenization buffer [in mM: 50 Tris (pH 8.0), 1 EDTA, 1 EGTA, 1 dithiothreitol, and 200 sucrose] with protease inhibitors (Complete Mini, Roche, Basel, Switzerland). Protein content was determined using the Coomassie Plus protein assay (Pierce Chemical, Rockford, IL), and BSA (0.1–1 mg/ml) was used as a standard. The protein samples (20 μg) were separated in the same gel by SDS-polyacrylamide gel electrophoresis and transferred to polyvinylidene difluoride membranes (Bio-Rad, Hercules, CA). When the molecular size of target proteins was different, polyvinylidene difluoride membranes were cut in accordance with their size. When the molecular size of target proteins was similar, we reused the same membrane for a different antibody after washing the membrane with a stripping buffer [in mM: 62.5 Tris (pH 8.0), 100 2-mercaptoethanol, and 2% SDS]. Antibodies used in the present study are shown in Supplemental Table 1. After application of a secondary antibody, quantification of the target signals was performed using the LAS-3000 imaging system (FUJIFILM, Tokyo, Japan). The protein levels of interest were normalized to rat β-actin. For reuse, a membrane was washed with a stripping buffer at 55°C for 10 min and was washed three times with 0.1% Tris buffered saline-Tween 20 buffer.

SR Ca^{2+}-ATPase assay. SR Ca^{2+}-ATPase activity was measured in triplicate spectrophotometrically at 37°C, as described previously with some modifications (18). Briefly, using 5 μg of SR protein from mice heart tissues, the reaction was carried out at 37°C in a reaction medium [in mM: 30 TES, 100 KCl, 5 NaN_3, 5 $MgCl_2$, 0.5 EGTA, and 4 ATP, with or without 0.5 $CaCl_2$]. The reaction medium was preincubated at 37°C for 5 min. The reaction was started at 37°C by adding SR protein to the medium. After 5 min, the reaction was stopped by adding 0.5 ml of ice-cold 10% trichloroacetic acid solution, and the mixture was placed on ice. Inorganic phosphate was measured by using U2001 (Hitachi), as described previously (8). Ca^{2+}-ATPase activity was calculated by subtracting the ATPase activity in the presence of 0.5 mM EGTA (no added Ca^{2+}) from the activity in the presence of 0.5 mM $CaCl_2$.

Statistical analysis. All values are expressed as means ± SE. Comparisons of data from multiple groups were performed by unpaired ANOVA followed by the Student Newman-Keuls post hoc test. Statistical significance was defined as $P < 0.05$.

RESULTS

Effects of endurance exercise training on exercise ability in SARKO mice. Before the start of endurance exercise training, exercise ability was examined in WT and SARKO mice by a treadmill-based exercise stress test, described above. Maximal exercise ability, as evaluated by maximal belt speed, was lower in SARKO mice (n = 16, 65.0 ± 3.6 cm/s) than in WT mice

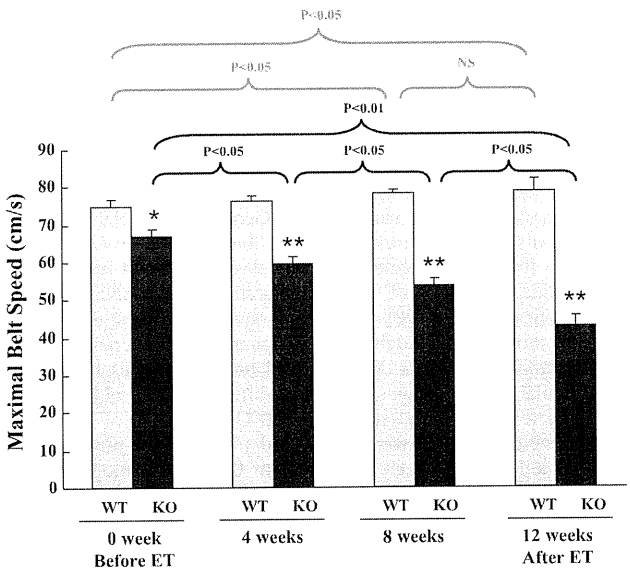

Fig. 1. The effect of endurance exercise training (ET) on maximal exercise ability in sarcalumenin (SAR) knockout (SARKO) mice. Maximal exercise ability, as evaluated by maximal belt speed, is already lower in SARKO mice than in wild-type (WT) mice before ET. During ET, maximal exercise ability gradually increased in WT mice, whereas it actually decreased in SARKO mice in a time-dependent manner. Maximal exercise ability after ET was significantly increased in WT mice, whereas it was actually decreased in SARKO mice compared with their maximal exercise ability before the training. Values are means ± SE; n = 6 and 5 for WT and knockout (KO), respectively.

(n = 16, 74.1 ± 2.1 cm/s), although it did not reach a statistical significance (P = 0.059). As expected, maximal exercise ability in sedentary animals (SED-WT and SED-SARKO mice) did not significantly change during the 12-wk training period (data not shown). In ET-WT mice, maximal exercise ability gradually increased during endurance exercise training, whereas, in ET-SARKO mice, it gradually decreased (Fig. 1). Whenever a change in a mouse's maximal exercise ability was detected by a regular treadmill test, that mouse's training workload was adjusted based on its current maximal speed (Supplemental Fig. 1). Maximal exercise ability after endurance exercise training significantly increased by 5% in ET-WT mice, whereas it actually decreased by 37% in ET-SARKO mice compared with their ability measured before the training regime began (Fig. 1).

Exercise training did not improve CS activity in SARKO mice. We observed no difference between WT and SARKO mice in terms of CS activity of skeletal or cardiac muscle at a basal condition. After the endurance exercise training, ET-WT mice exhibited increased CS activity of soleus muscle (Fig. 2*A*), indicating an appropriate effect of the training program on working muscles. In accordance, they also exhibited increased CS activity of cardiac muscle (Fig. 2*B*), which is consistent with several previous studies (1, 20), although most of previous studies have demonstrated that CS activity is not increased or little increased by endurance exercise in rodent hearts (4, 19). In ET-SARKO mice, on the other hand, CS activity was not increased in either soleus or cardiac muscle (Fig. 2).

Endurance exercise training resulted in cardiac dysfunction in SARKO mice. To examine the effect of endurance exercise training on cardiac function, we investigated it using transthoracic echocardiography. Before endurance exercise training, all parameters listed in Table 1 were similar between WT and SARKO mice, including body weight, heart rate, left ventricular fractional shortening, thickness of myocardial walls, and ejection time. After endurance exercise training, left ventricular fractional shortening was significantly decreased in ET-SARKO mice, whereas it was not changed in ET-WT mice (Table 1). As we expected, the diameter of the end-diastolic left ventricular chamber was significantly increased in ET-SARKO mice. Furthermore, ejection time was significantly prolonged in ET-SARKO mice, and their heart rate corrected velocity of circumferential fiber shortening was significantly lower (Table 1).

Biomarkers of cardiac stress were increased in ET-SARKO hearts. To examine the effect of endurance exercise training on the myocardium itself, we measured molecular markers of

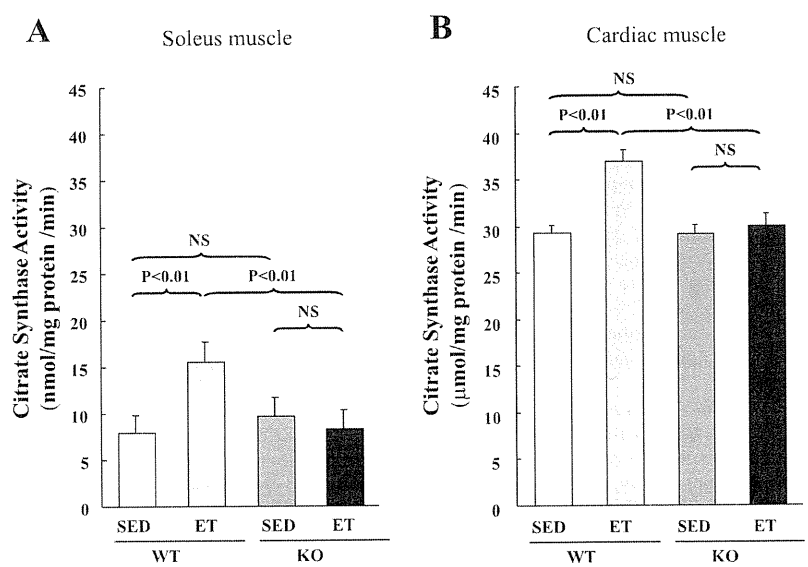

Fig. 2. Citrate synthase (CS) activity after ET. After ET, CS activity of soleus muscle (*A*) and cardiac muscle (*B*) was increased in ET-WT mice, but not in ET-SARKO mice. Values are means ± SE; n = 5 for each group. SED, sedentary; NS, not significant.

Table 1. *Cardiac function after endurance exercise training*

	SED-WT		ET-WT		SED-SARKO		ET-SARKO	
	Pre	Post	Pre	Post	Pre	Post	Pre	Post
n	10	10	6	6	10	10	6	5
BW, g	24.2±1.3	32.6±1.9	26.3±1.7	31.1±1.3	23.3±1.0	27.3±1.1	22.6±1.2	26.3±1.8
HR, beats/min	464±15	474±15	438±18	436±18	430±12	409±14	449±24	425±14
LV weight, mg		115±9		111±7		93±6		86±7
LV-to-BW weight ratio, mg/g		3.55±0.25		3.58±0.15		3.38±0.12		3.26±0.15
LV FS, %	35.6±1.1	35.5±1.0	34.7±1.2	34.9±2.6	37.5±1.3	34.0±1.2	38.6±2.7	28.4±1.1[a,c,d]
LVIDd, mm	4.11±0.08	4.12±0.11	4.03±0.06	4.25±0.12	3.88±0.10	4.02±0.09	3.84±0.12	4.14±0.19[a]
IVSTd, mm	0.77±0.03	0.79±0.05	0.77±0.02	0.71±0.05	0.76±0.02	0.67±0.01[b]	0.76±0.02	0.66±0.02[b]
LVPWTd, mm	0.76±0.03	0.75±0.04	0.76±0.04	0.76±0.06	0.72±0.07	0.65±0.04[a]	0.69±0.02	0.67±0.02[a,c]
Ejection time, ms	60±1	60±1	64±2	66±3	64±2	65±2	58±2	69±3[a]
Vcfc, circumferences/s	2.14±0.06	2.13±0.07	2.12±0.10	2.14±0.17	2.21±0.10	2.04±0.14	2.44±0.18	1.56±0.05[b,c,d]

Values are means ± SE; *n*, no. of mice. SED, sedentary; WT, wild-type mice; ET, endurance exercise training; SARKO, sarcalumenin-knockout mice; Pre, before ET; Post, after ET; BW, body weight; HR, heart rate; LV, left ventricle; FS, fractional shortening; LVIDd, LV internal dimensions at end diastole; IVSTd, interventricular septum thickness at end diastole; LVPWTd, LV posterior wall thickness at end diastole; Vcfc, corrected velocity of circumferential fiber shortening. Significant difference vs. Pre: [a]$P < 0.05$ and [b]$P < 0.01$; vs. WT: [c]$P < 0.05$; and vs. SED: [d]$P < 0.05$.

cardiac stress, such as ANF and BNP mRNAs. These were significantly upregulated in ET-SARKO mice (Fig. 3). Endurance training did not affect the expression of ANF and BNP mRNAs in ET-WT mice.

Significant reductions in the expression of Ca^{2+} handling proteins in ET-SARKO mice. Since the expression levels of SERCA2a and other Ca^{2+} handling proteins are critical for the regulation of cardiac function, we examined them by Western blot analyses (Fig. 4, Table 2). Consistent with our laboratory's previous report (26, 38), the expression levels of SERCA2a and total PLN were significantly downregulated in SED-SARKO mice compared with those in SED-WT mice. After endurance exercise training, the expression level of SERCA2a protein was significantly increased by 59% in ET-WT mice, whereas it was reduced by 30% in ET-SARKO mice compared with sedentary mice of each group's respective genotype. Endurance exercise training also resulted in a further significant downregulation of both total and phosphorylated PLN proteins in ET-SARKO mice, but not in ET-WT mice. The SERCA2a-to-PLN protein ratio was significantly decreased in ventricular muscles of ET-SARKO mice (Table 2). The ratio of phosphorylated threonine 17 PLN to total PLN protein was significantly lower in ET-SARKO than in ET-WT, but that of serine 16 to total PLN protein was not (Table 2). It should be noted that intraperitoneal injection of Avertin did not affect the phosphorylation status of serine 16 and threonine 17 in PLN (Supplemental Fig. 2).

The expression levels of calsequestrin 2 (CSQ2) and ryanodine receptor type 2 (RyR2) proteins in SED-SARKO mice were comparable to those in SED-WT mice, while those of sodium/calcium exchanger 1 (NCX1) protein were even higher in SED-SARKO mice than in SED-WT mice. After the endurance exercise training, all of these proteins were significantly downregulated in ET-SARKO mice, but not in ET-WT mice (Fig. 4, Table 2). Overall, in addition to SERCA2, all other Ca^{2+} handling proteins that we examined were downregulated in ET-SARKO mice after endurance exercise training.

Significant reduction in SERCA2a activity in ET-SARKO mice. As measured in myocardial homogenates, maximal Ca^{2+}-ATPase activity was lower in SED-SARKO mice than in SED-WT mice (Fig. 5). After the endurance exercise training, maximal Ca^{2+}-ATPase activity was further significantly decreased in ET-SARKO mice, whereas it was significantly increased in ET-WT mice. This result was consistent with the change in the ratio of SERCA2a to PLN protein expression shown in Table 2.

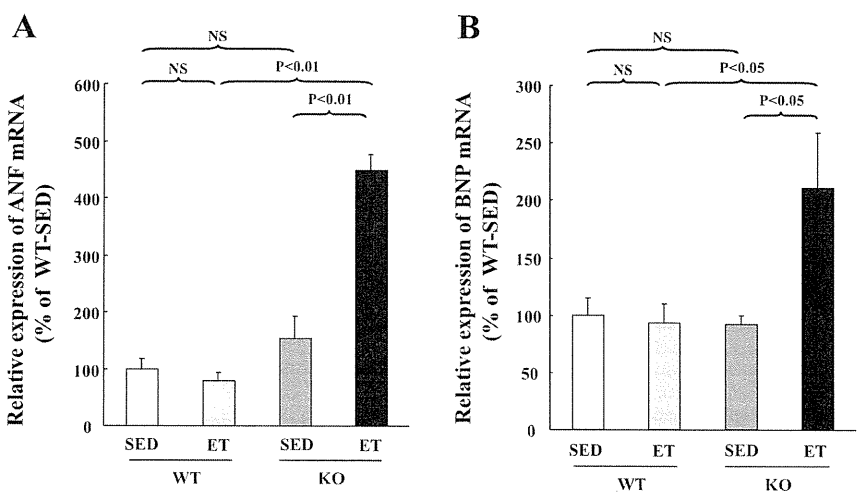

Fig. 3. Upregulation of atrial natriuretic factor (ANF) and brain natriuretic peptide (BNP) mRNAs in ET-SARKO mice. Quantitative RT-PCR analyses revealed that the expression levels of ANF (*A*) and BNP (*B*) mRNAs were significantly upregulated in the ventricles of ET-SARKO mice. The expression levels observed in SED-WT mice were set as 100% as a control. mRNA expression was normalized by GAPDH. Values are means ± SE; $n = 5$ for each group.

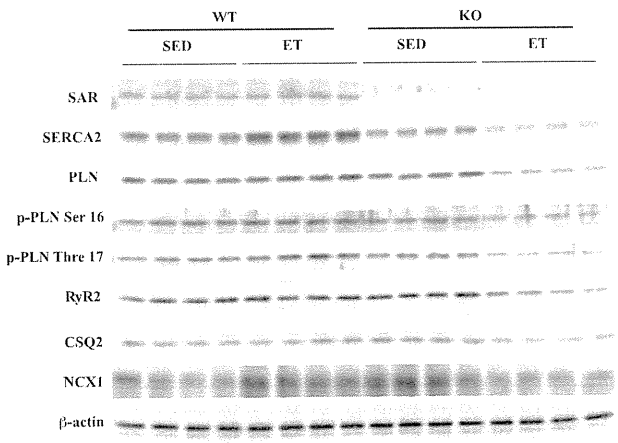

Fig. 4. The expression of Ca^{2+} handling proteins after ET. The expression levels of sarcalumenin (SAR), sarco(endo)plasmic reticulum Ca^{2+}-ATPase 2 (SERCA2), phospholamban (PLN), phosphorylated PLN (p-PLN), ryanodine receptor 2 (RyR2), calsequestrin 2 (CSQ2), and sodium/calcium exchanger 1 (NCX1) proteins were quantified in hearts isolated from SED and ET mice. Protein expression was normalized by β-actin.

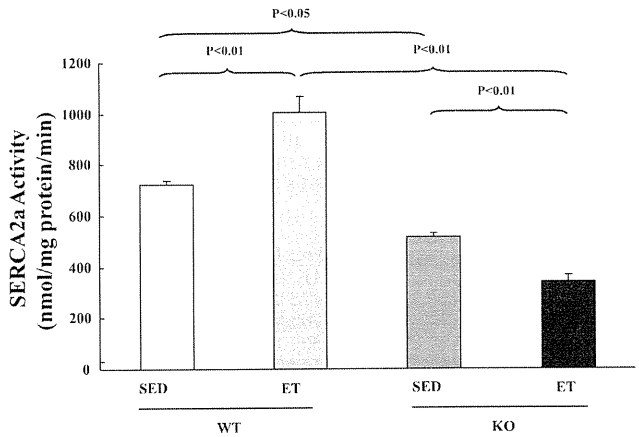

Fig. 5. SERCA2a activity after ET. SERCA2a activity was increased in ET-WT, whereas it was decreased in ET-SARKO after ET. Values are means ± SE; $n = 5$ for each group.

DISCUSSION

The most striking finding in the present study is that long-term (12 wk) endurance exercise training induced a significant cardiac dysfunction in mice that harbor systemic ablation of the SAR gene. Along the same lines, we have recently demonstrated that SARKO mice failed to adapt to pressure-overloaded stress induced by transverse aortic constriction (26), whereas sedentary young SARKO mice exhibit mild cardiac dysfunction (38). Since exercise is one of the most common physiological stresses, the present data indicate that SAR plays an important role in preserving cardiac function during adaptation to not only pathological, but also physiological, stresses.

It should be noted that the absolute training intensity undertaken by SARKO mice was significantly lower than that undertaken by WT mice (Supplemental Fig. 1), because the intensity of each mouse's exercise regime was determined on the basis of that mouse' maximal exercise ability. Accordingly, CS activity in soleus muscle after endurance exercise training was significantly lower in ET-SARKO mice than in ET-WT mice (Fig. 2). Since skeletal muscle CS activity is a marker for mitochondrial content (a hallmark of endurance exercise) and muscle oxidative capacity, this result indicates that our exercise training program is sufficient to enhance the exercise ability of WT mice, but insufficient to enhance that of SARKO mice. Although this may explain a number of the negative effects on SARKO mice that were caused by exercise training in the present study, it is, nevertheless, very difficult to explain why ET-SARKO mice exhibited progressive cardiac dysfunction. We assume that inadequate adaptation to endurance exercise in ET-SARKO mice caused impaired cardiac function, the primary insult, which, secondarily, resulted in a number of negative effects on SARKO mice caused by training.

Table 2. *The expression of calcium handling proteins after endurance exercise training*

	SED-WT	ET-WT	SED-SARKO	ET-SARKO
SAR	100±5	108±9		
SERCA2	100±10	159±13§	74±4*	52±6†‡
PLN	100±6	123±8	83±2*	71±2†§
p-PLN Ser 16	100±3	120±11	95±5	82±3†‡
p-PLN Thre 17	100±4	112±7	92±6	78±4†‡
SERCA2/PLN	100±5	132±12‡	94±4	75±10†‡
p-PLN Ser 16/PLN	100±4	98±8	113±4	116±8
p-PLN Thre 17/PLN	100±1	98±4	93±2	88±2*
RyR2	100±5	100±10	97±6	68±8*‡
CSQ2	100±7	101±4	99±3	83±6*‡
NCX1	100±10	139±11‡	124±3*	92±11*‡

Values are means ± SE; $n = 5$ mice for each group. The expression level in SED-WT mice was referred to 100% as a control. Protein expression was normalized by β-actin. SAR, sarcalumenin; SERCA2, sarco(endo)plasmic reticulum Ca^{2+}-ATPase 2; PLN, phospholamban; p-PLN: phosphorylated phospholamban; RyR2, ryanodine receptor 2; CSQ2, calsequestrin 2; NCX1, sodium/calcium exchanger 1. Significant difference vs. WT: *$P < 0.05$ and †$P < 0.01$; vs. SED: ‡$P < 0.05$ and §$P < 0.01$.

The mechanism by which endurance exercise induced progressive cardiac dysfunction in SARKO mice is a critical question. One observation that may be relevant to this question is the significant decrease in the expression and activity of SERCA2a in ET-SARKO mice. A number of previous studies have reported that endurance exercise training increased the expression and/or activity of SERCA2a in healthy (9, 10, 20, 22, 30, 35) or diseased rodents (6, 21, 24, 34, 39); similarly, we found that the expression and activity of SERCA2a increased after endurance exercise training in control mice. Yet other studies have demonstrated that endurance exercise training does not change the expression and/or activity of SERCA2a (3, 4) or Ca^{2+} transients (12) in rodents. It is worth noting that these conflicting results may have their origins in such factors as differences in species, exercise protocols, and/or condition of the subjects; few studies, however, have shown that endurance exercise decreases the expression and/or activity of SERCA2a. Therefore, our results found in ET-SARKO mice were so remarkable that it is very important to investigate why SAR deficiency caused the significant reduction in the expression and activity of SERCA2a under endurance exercise training.

Our laboratory's recent study has demonstrated that SAR interacts with SERCA2 to enhance the protein stability of SERCA2a (26). Since exercise training usually increases pro-

tein synthesis and degradation in muscle (11, 23), we assume that endurance exercise training also increased the turnover rate of SERCA2a protein. Then we postulate that SAR deficiency induced a progressive degradation of SERCA2a protein due to impaired protein stabilization under endurance exercise training and resulted in the significant decrease in the expression of SERCA2a in ET-SARKO mice. Importantly, the present study demonstrated that endurance exercise training slightly increased the expression levels of SAR protein in WT hearts, in accordance with a significant increase in the expression of SERCA2a protein. To our knowledge, this is the first report to show the effect of endurance exercise training on the expression of SAR protein. These data suggest that SAR is a key regulatory protein to maintain the expression level of SERCA2a protein under pathophysiological stresses. In addition, the ratios of SERCA2a to PLN protein and phosphorylated threonine 17 PLN to total PLN protein were significantly decreased in the ventricular muscles of ET-SARKO mice, indicating that SERCA2a activity was inhibited by PLN more in ET-SARKO mice than in other groups. Taken together, this evidence shows that SAR deficiency induced a significant reduction in SERCA2a activity and deterioration of the Ca^{2+} storage system in the SR under endurance exercise stress, which is very likely to play a primary role in the exercise-induced cardiac dysfunction exhibited by ET-SARKO mice.

Interestingly, in addition to the decreases in the SERCA2a and PLN proteins that interact with SAR in the longitudinal SR, other Ca^{2+} handling proteins, such as RyR2, CSQ2, and NCX1, were also significantly downregulated in ET-SARKO mice, which has not been investigated in pressure-overloaded SARKO hearts (26). These abnormalities probably contribute to the further impairment of cardiac function during endurance exercise training. We assume that the downregulation of RyR2, CSQ2, and NCX1 could be a secondary phenomenon that occurs under physiological stress conditions, as SAR does not directly interact with these proteins. The mechanism of these discrepant responses to different stresses in SARKO mice is currently not clear; it is an important question that should be addressed in future studies.

In one way, the results of the present study somehow contradict those of a recent report by Zhao et al. (40), which showed that skeletal muscles from SARKO mice are highly resistant to fatigue compared with those from WT mice. The same authors have also demonstrated that SOCE was promoted in SARKO skeletal muscle by the upregulation of MG29 (40). They proposed that the promotion of SOCE played a role in making skeletal muscle more fatigue resistant (40). In the present study, however, we did not detect any expression of MG29 protein in either WT or SARKO hearts, before or after exercise training, although we used the same membranes for our Western blot analyses (data not shown). This observation is consistent with a previous study (29). Currently, we cannot explain the exact reason for the disagreement between the results of Zhao et al. (40) and our own. A possible explanation is the difference in the exercise programs our two groups used to evaluate the exercise performance of SARKO mice. Further investigation is needed to clarify whether a defect of MG29 may cause the negative responses to exercise in SARKO cardiac muscle cells.

In conclusion, we found that cardiac function and maximal exercise ability were significantly impaired in SARKO mice after endurance treadmill exercise training. These impairments were due, at least in part, to a significant downregulation of SERCA2a and other Ca^{2+} handling proteins and to a deterioration of the Ca^{2+} storage system in the SARKO heart under endurance exercise. Thus present study indicates that SAR plays a critical role in maintaining cardiac function under physiological stresses, such as endurance exercise, by regulating Ca^{2+} transport activity into the SR. SAR may be a primary target for exercise-related adaptation of the Ca^{2+} storage system in the SR to preserve cardiac function.

GRANTS

This work was partly supported by grants from the Honjo International Scholarship Foundation (Q. Jiao), the Yokohama Foundation for Advanced Medical Science (S. Minamisawa, T. Akaike, Y. Ishikawa), the Ministry of Education, Science, Sports and Culture of Japan (S. Minamisawa, Y. Ishikawa), the Special Coordination Funds for Promoting Science and Technology, MEXT (S. Minamisawa), the "High-Tech Research Center" Project for Private Universities: matching fund subsidy from MEXT (S. Minamisawa), a Waseda University Grant for Special Research Projects (S. Minamisawa), the Mother and Child Health Foundation (S. Minamisawa), the Miyata Cardiology Research Promotion Funds (S. Minamisawa), the Takeda Science Foundation (S. Minamisawa), the Foundation for Growth Science (S. Minamisawa), the Japan Cardiovascular Research Foundation (S. Minamisawa), the Mitsubishi Pharma Research Foundation (S. Minamisawa), the Yokohama Academic Foundation (T. Akaike), the Inoue Foundation for Science (T. Akaike), the Naito Foundation (T. Akaike), the Japan Space Forum (Y. Ishikawa), and the National Institute of General Medical Sciences (RO1 GM067773) (Y. Ishikawa).

REFERENCES

1. **Call JA, Voelker KA, Wolff AV, McMillan RP, Evans NP, Hulver MW, Talmadge RJ, Grange RW.** Endurance capacity in maturing mdx mice is markedly enhanced by combined voluntary wheel running and green tea extract. *J Appl Physiol* 105: 923–932, 2008.
2. **Charlton GA, Crawford MH.** Physiologic consequences of training. *Cardiol Clin* 15: 345–354, 1997.
3. **de Waard MC, van der Velden J, Bito V, Ozdemir S, Biesmans L, Boontje NM, Dekkers DH, Schoonderwoerd K, Schuurbiers HC, de Crom R, Stienen GJ, Sipido KR, Lamers JM, Duncker DJ.** Early exercise training normalizes myofilament function and attenuates left ventricular pump dysfunction in mice with a large myocardial infarction. *Circ Res* 100: 1079–1088, 2007.
4. **Delgado J, Saborido A, Moran M, Megias A.** Chronic and acute exercise do not alter Ca^{2+} regulatory systems and ectonucleotidase activities in rat heart. *J Appl Physiol* 87: 152–160, 1999.
5. **Frank KF, Bolck B, Erdmann E, Schwinger RH.** Sarcoplasmic reticulum Ca^{2+}-ATPase modulates cardiac contraction and relaxation. *Cardiovasc Res* 57: 20–27, 2003.
6. **French JP, Quindry JC, Falk DJ, Staib JL, Lee Y, Wang KK, Powers SK.** Ischemia-reperfusion-induced calpain activation and SERCA2a degradation are attenuated by exercise training and calpain inhibition. *Am J Physiol Heart Circ Physiol* 290: H128–H136, 2006.
7. **Houser SR, Piacentino V 3rd, Weisser J.** Abnormalities of calcium cycling in the hypertrophied and failing heart. *J Mol Cell Cardiol* 32: 1595–1607, 2000.
8. **Hwang KJ.** Interference of ATP and acidity in the determination of inorganic phosphate by the Fiske and Subbarow method. *Anal Biochem* 75: 40–44, 1976.
9. **Iemitsu M, Miyauchi T, Maeda S, Tanabe T, Takanashi M, Matsuda M, Yamaguchi I.** Exercise training improves cardiac function-related gene levels through thyroid hormone receptor signaling in aged rats. *Am J Physiol Heart Circ Physiol* 286: H1696–H1705, 2004.
10. **Kemi OJ, Ceci M, Condorelli G, Smith GL, Wisloff U.** Myocardial sarcoplasmic reticulum Ca^{2+} ATPase function is increased by aerobic interval training. *Eur J Cardiovasc Prev Rehabil* 15: 145–148, 2008.
11. **Kumar V, Atherton P, Smith K, Rennie MJ.** Human muscle protein synthesis and breakdown during and after exercise. *J Appl Physiol* 106: 2026–2039, 2009.

12. **Laughlin MH, Schaefer ME, Sturek M.** Effect of exercise training on intracellular free Ca^{2+} transients in ventricular myocytes of rats. *J Appl Physiol* 73: 1441–1448, 1992.
13. **Leberer E, Charuk JH, Green NM, MacLennan DH.** Molecular cloning and expression of cDNA encoding a lumenal calcium binding glycoprotein from sarcoplasmic reticulum. *Proc Natl Acad Sci USA* 86: 6047–6051, 1989.
14. **Levy WC, Cerqueira MD, Abrass IB, Schwartz RS, Stratton JR.** Endurance exercise training augments diastolic filling at rest and during exercise in healthy young and older men. *Circulation* 88: 116–126, 1993.
15. **Lu L, Mei DF, Gu AG, Wang S, Lentzner B, Gutstein DE, Zwas D, Homma S, Yi GH, Wang J.** Exercise training normalizes altered calcium-handling proteins during development of heart failure. *J Appl Physiol* 92: 1524–1530, 2002.
16. **MacLennan DH, Wong PT.** Isolation of a calcium-sequestering protein from sarcoplasmic reticulum. *Proc Natl Acad Sci USA* 68: 1231–1235, 1971.
17. **Minamisawa S, Sato Y, Cho MC.** Calcium cycling proteins in heart failure, cardiomyopathy and arrhythmias. *Exp Mol Med* 36: 193–203, 2004.
18. **Minamisawa S, Wang Y, Chen J, Ishikawa Y, Chien KR, Matsuoka R.** Atrial chamber-specific expression of sarcolipin is regulated during development and hypertrophic remodeling. *J Biol Chem* 278: 9570–9575, 2003.
19. **Moore RL.** Cellular adaptations of the heart muscle to exercise training. *Ann Med* 30, *Suppl* 1: 46–53, 1998.
20. **Moran M, Saborido A, Megias A.** Ca^{2+} regulatory systems in rat myocardium are altered by 24 weeks treadmill training. *Pflügers Arch* 446: 161–168, 2003.
21. **Mou YA, Reboul C, Andre L, Lacampagne A, Cazorla O.** Late exercise training improves non-uniformity of transmural myocardial function in rats with ischaemic heart failure. *Cardiovasc Res* 81: 555–564, 2009.
22. **Pierce GN, Sekhon PS, Meng HP, Maddaford TG.** Effects of chronic swimming training on cardiac sarcolemmal function and composition. *J Appl Physiol* 66: 1715–1721, 1989.
23. **Pikosky MA, Gaine PC, Martin WF, Grabarz KC, Ferrando AA, Wolfe RR, Rodriguez NR.** Aerobic exercise training increases skeletal muscle protein turnover in healthy adults at rest. *J Nutr* 136: 379–383, 2006.
24. **Rolim NP, Medeiros A, Rosa KT, Mattos KC, Irigoyen MC, Krieger EM, Krieger JE, Negrao CE, Brum PC.** Exercise training improves the net balance of cardiac Ca^{2+} handling protein expression in heart failure. *Physiol Genomics* 29: 246–252, 2007.
25. **Seals DR, Hagberg JM, Spina RJ, Rogers MA, Schechtman KB, Ehsani AA.** Enhanced left ventricular performance in endurance trained older men. *Circulation* 89: 198–205, 1994.
26. **Shimura M, Minamisawa S, Takeshima H, Jiao Q, Bai Y, Umemura S, Ishikawa Y.** Sarcalumenin alleviates stress-induced cardiac dysfunction by improving Ca^{2+} handling of the sarcoplasmic reticulum. *Cardiovasc Res* 77: 362–370, 2008.
27. **Singh M, Brooks GC, Srere PA.** Subunit structure and chemical characteristics of pig heart citrate synthase. *J Biol Chem* 245: 4636–4640, 1970.
28. **Tadano M, Edamatsu H, Minamisawa S, Yokoyama U, Ishikawa Y, Suzuki N, Saito H, Wu D, Masago-Toda M, Yamawaki-Kataoka Y, Setsu T, Terashima T, Maeda S, Satoh T, Kataoka T.** Congenital semilunar valvulogenesis defect in mice deficient in phospholipase C epsilon. *Mol Cell Biol* 25: 2191–2199, 2005.
29. **Takeshima H, Shimuta M, Komazaki S, Ohmi K, Nishi M, Iino M, Miyata A, Kangawa K.** Mitsugumin29, a novel synaptophysin family member from the triad junction in skeletal muscle. *Biochem J* 331: 317–322, 1998.
30. **Tate CA, Helgason T, Hyek MF, McBride RP, Chen M, Richardson MA, Taffet GE.** SERCA2a and mitochondrial cytochrome oxidase expression are increased in hearts of exercise-trained old rats. *Am J Physiol Heart Circ Physiol* 271: H68–H72, 1996.
31. **Thomas DP.** Effects of acute and chronic exercise on myocardial ultrastructure. *Med Sci Sports Exerc* 17: 546–553, 1985.
32. **Trounce IA, Kim YL, Jun AS, Wallace DC.** Assessment of mitochondrial oxidative phosphorylation in patient muscle biopsies, lymphoblasts, and transmitochondrial cell lines. *Methods Enzymol* 264: 484–509, 1996.
33. **Ventura-Clapier R, Mettauer B, Bigard X.** Beneficial effects of endurance training on cardiac and skeletal muscle energy metabolism in heart failure. *Cardiovasc Res* 73: 10–18, 2007.
34. **Wisloff U, Loennechen JP, Currie S, Smith GL, Ellingsen O.** Aerobic exercise reduces cardiomyocyte hypertrophy and increases contractility, Ca^{2+} sensitivity and SERCA-2 in rat after myocardial infarction. *Cardiovasc Res* 54: 162–174, 2002.
35. **Wisloff U, Loennechen JP, Falck G, Beisvag V, Currie S, Smith G, Ellingsen O.** Increased contractility and calcium sensitivity in cardiac myocytes isolated from endurance trained rats. *Cardiovasc Res* 50: 495–508, 2001.
36. **Yokoyama U, Minamisawa S, Adachi-Akahane S, Akaike T, Naguro I, Funakoshi K, Iwamoto M, Nakagome M, Uemura N, Hori H, Yokota S, Ishikawa Y.** Multiple transcripts of Ca^{2+} channel α1-subunits and a novel spliced variant of the α1C-subunit in rat ductus arteriosus. *Am J Physiol Heart Circ Physiol* 290: H1660–H1670, 2006.
37. **Yokoyama U, Minamisawa S, Quan H, Ghatak S, Akaike T, Segi-Nishida E, Iwasaki S, Iwamoto M, Misra S, Tamura K, Hori H, Yokota S, Toole BP, Sugimoto Y, Ishikawa Y.** Chronic activation of the prostaglandin receptor EP4 promotes hyaluronan-mediated neointimal formation in the ductus arteriosus. *J Clin Invest* 116: 3026–3034, 2006.
38. **Yoshida M, Minamisawa S, Shimura M, Komazaki S, Kume H, Zhang M, Matsumura K, Nishi M, Saito M, Saeki Y, Ishikawa Y, Yanagisawa T, Takeshima H.** Impaired Ca^{2+} store functions in skeletal and cardiac muscle cells from sarcalumenin-deficient mice. *J Biol Chem* 280: 3500–3506, 2005.
39. **Zhang LQ, Zhang XQ, Ng YC, Rothblum LI, Musch TI, Moore RL, Cheung JY.** Sprint training normalizes Ca^{2+} transients and SR function in postinfarction rat myocytes. *J Appl Physiol* 89: 38–46, 2000.
40. **Zhao X, Yoshida M, Brotto L, Takeshima H, Weisleder N, Hirata Y, Nosek TM, Ma J, Brotto M.** Enhanced resistance to fatigue and altered calcium handling properties of sarcalumenin knockout mice. *Physiol Genomics* 23: 72–78, 2005.

THE JOURNAL OF BIOLOGICAL CHEMISTRY VOL. 284, NO. 36, pp. 24025–24034, September 4, 2009

T-type Ca^{2+} Channels Promote Oxygenation-induced Closure of the Rat Ductus Arteriosus Not Only by Vasoconstriction but Also by Neointima Formation*[S]

Received for publication, May 8, 2009, and in revised form, June 24, 2009 Published, JBC Papers in Press, June 30, 2009, DOI 10.1074/jbc.M109.017061

Toru Akaike[‡], Mei-Hua Jin[‡], Utako Yokoyama[‡], Hiroko Izumi-Nakaseko[§], Qibin Jiao[‡], Shiho Iwasaki[¶], Mari Iwamoto[¶], Shigeru Nishimaki[¶], Motohiko Sato[‡], Shumpei Yokota[¶], Yoshinori Kamiya[‖], Satomi Adachi-Akahane[§], Yoshihiro Ishikawa[‡], and Susumu Minamisawa[‡ ‡‡§§1]**

*From the [‡]Cardiovascular Research Institute, Yokohama City University Graduate School of Medicine, Yokohama 236-0004, Japan, the [§]Department of Pharmacology, School of Medicine, Faculty of Medicine, Graduate School of Medical Sciences, Toho University, Toho 143-8540, Japan, the [¶]Department of Pediatrics, Yokohama City University Graduate School of Medicine, Yokohama 236-0004, Japan, the [‖]Department of Anesthesiology, Yokohama City University Graduate School of Medicine, Yokohama 236-0004, Japan, the **Cardiovascular Research Institute, Departments of Cell Biology & Molecular Medicine and Medicine (Cardiology), New Jersey Medical School, Newark, New Jersey 07101-1709, the [‡‡]Department of Life Science and Medical Bioscience, Waseda University, Tokyo 162-8480, Japan, and the [§§]Institute for Biomedical Engineering, Consolidated Research Institute for Advanced Science and Medical Care, Waseda University, Tokyo 162-8480, Japan*

The ductus arteriosus (DA), an essential vascular shunt for fetal circulation, begins to close immediately after birth. Although Ca^{2+} influx through several membrane Ca^{2+} channels is known to regulate vasoconstriction of the DA, the role of the T-type voltage-dependent Ca^{2+} channel (VDCC) in DA closure remains unclear. Here we found that the expression of α1G, a T-type isoform that is known to exhibit a tissue-restricted expression pattern in the rat neonatal DA, was significantly up-regulated in oxygenated rat DA tissues and smooth muscle cells (SMCs). Immunohistological analysis revealed that α1G was localized predominantly in the central core of neonatal DA at birth. DA SMC migration was significantly increased by α1G overexpression. Moreover, it was decreased by adding α1G-specific small interfering RNAs or using $R(-)$-efonidipine, a highly selective T-type VDCC blocker. Furthermore, an oxygenation-mediated increase in an intracellular Ca^{2+} concentration of DA SMCs was significantly decreased by adding α1G-specific siRNAs or using $R(-)$-efonidipine. Although a prostaglandin E receptor EP4 agonist potently promoted intimal thickening of the DA explants, $R(-)$-efonidipine (10^{-6} M) significantly inhibited EP4-promoted intimal thickening by 40% using DA tissues at preterm in organ culture. Moreover, $R(-)$-efonidipine (10^{-6} M) significantly attenuated oxygenation-induced vasoconstriction by ~27% using a vascular ring of fetal DA at term. Finally, $R(-)$-efonidipine significantly delayed the closure of *in vivo* DA in neonatal rats. These results indicate that T-type VDCC, especially α1G, which is predominantly expressed in neonatal DA, plays a unique role in DA closure, implying that T-type VDCC is an alternative therapeutic target to regulate the patency of DA.

The ductus arteriosus (DA)[2] is an essential vascular shunt between the aortic arch and the pulmonary trunk during a fetal period (1). After birth, the DA closes immediately in accordance with its smooth muscle contraction and vascular remodeling, whereas the connecting vessels such as the aorta and pulmonary arteries remain open. When the DA fails to close after birth, the condition is known as patent DA, which is a common form of congenital heart defect. Patent DA is also a frequent problem with significant morbidity and mortality in premature infants. Investigating the molecular mechanism of DA closure is important not only for vascular biology but also for clinical problems in pediatrics.

Voltage-dependent Ca^{2+} channels (VDCCs) consist of multiple subtypes, named L-, N-, P/Q-, R-, and T-type. L-type VDCCs are known to play a primary role in regulating Ca^{2+} influx and thus vascular tone in the development of arterial smooth muscle including the DA (2–4). Our previous study demonstrated that all T-type VDCCs were expressed in the rat DA (5). α1G subunit, especially, was the most dominant isoform among T-type VDCCs. The abundant expression of α1G subunit suggests that it plays a role in the vasoconstriction and vascular remodeling of the DA. In this regard, Nakanishi

* This work was supported, in whole or in part, by National Institutes of Health Grant RO1 GM067773 (to Y. I.). This work was also supported by grants from the Yokohama Foundation for Advanced Medical Science (to T. A., U. Y., Y. I., and S. M.), the Ministry of Education, Culture, Sports, Science and Technology of Japan (to S. I., U. Y., Y. I., and S. M.), the Special Coordination Funds for Promoting Science and Technology, MEXT (to S. M.), "High-Tech Research Center" Project for Private Universities: matching fund subsidy from MEXT (to S. M.), Waseda University Grant for Special Research Projects (to S. M.), the Mother and Child Health Foundation (to S. M.), Miyata Cardiology Research Promotion Founds (to U. Y. and S. M.), Takeda Science Foundation (to S. M.), Foundation for Growth Science (to S. M.), Japan Cardiovascular Research Foundation (to S. M.), Mitsubishi Pharma Research Foundation (to S. M.), Yokohama Academic Foundation (to T. A. and S. I.), Inoue Foundation for Science (to T. A.), the Naito Foundation (to T. A.), the Uehara Memorial Foundation (to U. Y.), the Kitsuen Research Foundation (to Y. I.), and the Japan Space Forum (to Y. I.).

[S] The on-line version of this article (available at http://www.jbc.org) contains supplemental Figs. S1–S7.

[1] To whom correspondence should be addressed: Dept. of Life Science and Medical Bioscience, Waseda University Graduate School of Advanced Science and Engineering 2-2, Wakamatsu-cho, TWIns, Shinjuku-ku, Tokyo 162-8480, Japan. Tel.: 81-3-5369-7322; Fax: 81-3-5369-7022; E-mail: sminamis@waseda.jp.

[2] The abbreviations used are: DA, ductus arteriosus; VDCC, voltage-dependent Ca^{2+} channel; SMC, smooth muscle cell; siRNA, small interfering RNA; FCS, fetal calf serum; fura-2/AM, fura-2 acetoxymethyl ester.

et al. (6) demonstrated that 0.5 mM nickel, which blocks T-type VDCC, inhibited oxygen-induced vasoconstriction of the rabbit DA. On the other hand, Tristani-Firouzi *et al.* (7) demonstrated that T-type VDCCs exhibited little effect on oxygen-sensitive vasoconstriction of the rabbit DA. Thus, the role of T-type VDCCs in DA vasoconstriction has remained controversial.

In addition to their role in determining the contractile state, a growing body of evidence has demonstrated that T-type VDCCs play an important role in regulating differentiation (8, 9), proliferation (10–12), migration (13, 14), and gene expression (15) in vascular smooth muscle cells (SMCs). Hollenbeck *et al.* (16) and Patel *et al.* (17) demonstrated that nickel inhibited platelet-derived growth factor-BB-induced SMC migration. Rodman *et al.* (18) demonstrated that α1G promoted SMC proliferation in the pulmonary artery. The DA dramatically changes its morphology during development. Intimal cushion formation, a characteristic feature of vascular remodeling of the DA (19–21), involves many cellular processes: an increase in SMC migration and proliferation, production of hyaluronic acid under the endothelial layer, impaired elastin fiber assembly, and so on (1, 19, 21–23). Although our previous study demonstrated that T-type VDCCs are involved in smooth muscle cell proliferation in the DA (5), the role of T-type VDCCs in vascular remodeling of the DA has remained poorly understood.

In the present study, we hypothesized that T-type VDCCs, especially α1G subunit, associate with vascular remodeling and vasoconstriction in the DA. To test our hypothesis, we took full advantage of recent molecular and pharmacological developments. We chose the recently developed, highly selective T-type VDCC blocker *R*(−)-efonidipine instead of low dose nickel for our study. Selective inhibition or activation of α1G subunit was also obtained using small interfering RNA (siRNA) technology or by overexpression of the α1G subunit gene, respectively. We found that Ca^{2+} influx through T-type VDCCs promoted oxygenation-induced DA closure through SMC migration and vasoconstriction.

EXPERIMENTAL PROCEDURES

Animals—Timed pregnant Wistar rats were purchased from Japan SLC, Inc. (Shizuoka, Japan). The DA was obtained from rat fetuses on the 19th day of gestation (preterm) and on the 21st day of gestation (term) and from neonates within at least 6 h after delivery. The DAs on the 19th day of gestation remained immature, whereas they became mature on the 21st day of gestation. All of the animals were cared for in compliance with the guiding principles of the American Physiologic Society. The experiments were approved by the Ethical Committees on Animal Experiments of Waseda University and Yokohama City University School of Medicine.

Reagents—*R*(−)-Efonidipine, a highly selective T-type VDCC blocker, and ONO-AE1–329, a selective prostaglandin E receptor EP4 agonist, were provided by Nissan Chemical Industries, Ltd. (Saitama, Japan) and ONO Pharmaceutical Co. (Osaka, Japan), respectively. Nitrendipine, a selective L-type VDCC blocker, was purchased from Sigma-Aldrich. α1G plasmid was kindly provided by Dr. Lory at Université Montpellier (Montpellier, France). Collagenase II was from the Worthington Biochemical Corp. (Lakewood, NJ). Collagenase/dispase was purchased from Roche Applied Science. Fetal calf serum (FCS) was purchased from Invitrogen. Platelet-derived growth factor-BB and 10% buffered formalin were purchased from Wako Pure Chemical Industries, Ltd. (Osaka, Japan). Elastase type II-A, trypsin inhibitor type I-S, bovine serum albumin V, penicillin-streptomycin solution, Dulbecco's modified Eagle's medium, and Hanks' balanced salt solution were purchased from Sigma-Aldrich. Anti-α1G and anti-α-smooth muscle actin antibodies were purchased from Sigma-Aldrich. Anti-Ki-67 antibody was purchased from Dako.

Immunoblotting—To examine the expression of α1G protein after birth, we used pooled tissues obtained from one littermate of Wistar rat neonates on the day of birth. After excision, the tissues were immediately frozen in liquid nitrogen and stored at −80 °C until use. Immunoblotting was performed as described previously (5).

Tissue Staining and Immunohistochemistry—To demonstrate the immunoperoxidase of α1G subunit and Ki-67 in the rat DA, tissue staining and immunohistochemistry were carried out as previously explained (5, 21).

Primary Culture of Rat DA SMCs—Vascular SMCs in primary culture were obtained from the DAs of Wistar rat embryos on embryonic day 21, as described previously (5, 21). The confluent cells for four to six passages were used in the experiments. We checked that these cells were in a more differentiated state than the cells of primary isolations, although the cells for four to six passages were in a less differentiated state than DA tissues at term and adult aortic artery, when the differentiation state was determined by the expression of marker genes of SMC differentiation such as SM1, SM2, and SMemb (supplemental Fig. S1). Therefore, it should be noted that the phenotype of cultured DA SMCs was not completely the same as the contractile phenotype of tissues of the DA and aorta. To examine the effect of a change in oxygen tension, DA SMCs were cultured in a hypoxic chamber (1% O_2, 5% CO_2) and then transferred to a normoxic chamber (21% O_2, 5% CO_2).

SMC Migration Assay—The migration assay was performed using 24-well transwell culture inserts with polycarbonate membranes (8-μm pores; Corning Inc.) as described previously with some minor modifications (21). Using a fibronectin-coated membrane of a Boyden chamber, we examined an acute (~4 h) effect of T-type VDCC on SMC migration by overexpression of a α1G protein or by inhibition with *R*(−)-efonidipine or with α1G-specific siRNAs. To examine the effect of T-type VDCC on actively migrating SMCs, 10% FCS was used as a potent stimulator for SMC migration.

Transfection of Plasmid DNAs and siRNAs in DA SMCs—A full-length of rat α1G cDNA was ligated to pcDNA3.1 plasmid vector. Plasmid DNAs were purified using a High Pure plasmid isolation kit (Roche Applied Science) according to the manufacturer's instructions. Genome-ONE NEO, an inactivated, column-purified HVJ-E vector, was purchased from Ishihara Sangyo Co. Ltd.(Osaka, Japan). Plasmid DNAs were transfected according to the manufacturer's instructions.

Two double-standard 21-bp siRNAs to the selected region of α1G subunit cDNA were purchased from Qiagen. The anti-

sense siRNA sequences targeting α1G subunit were 5′-UAGCAUUGGACAGGAAUCGdTdA-3′ and 5′-UAAUGUGACGAGAAUGCGCdAdT-3′. AllStars negative control siRNA purchased from Qiagen was used as a control nonsilencing siRNA. siRNAs were transfected as previously described (21).

Quantitative Reverse Transcription-PCR Analysis—Both isolation of total RNA from pooled tissues or cultured SMCs and generation of cDNA and reverse transcription-PCR analysis for α1G subunit were carried out as described previously (5). The forward primer specific for α1G subunit was 5′-cctgatttctttcgcccag-3′. The reverse primer specific for α1G subunit was 5′-tggcaaaaggctctttcgtag-3′. The 5′ and 3′ primers specific for glyceraldehyde-3-phosphate dehydrogenase were 5′-cccatcaccatcttccaggagcg-3′ and 3′-gcagggatgatgttctgggctgcc-5′. The abundance of each gene was determined relative to internal control using a Quantitect primer assay (Qiagen). For each reverse transcription-PCR experiment that included a reverse transcription negative control, we confirmed that there was no amplification in any reaction.

Intracellular Ca^{2+} Concentration in DA SMCs—DA SMCs were loaded with fura-2/AM (Dojindo, Kumamoto, Japan) in a Tyrode solution (137 mM NaCl, 2.7 mM KCl, 1.4 mM $CaCl_2$, 5.6 mM glucose, 0.5 mM $MgCl_2$, 0.3 mM NaH_2PO_4, 12 mM $NaHCO_3$, pH7.4). The DA SMCs on a 96-well microplate (Nunc) were superfused with the solution containing 2.5 μM fura-2/AM for 20 min at 37 °C. After the dye loading, the loading buffer was then removed, and the cells were washed twice with loading buffer. DA SMCs were incubated for 24 h under the following conditions within the dye loading time: a humidified chamber, 5% CO_2, and 1% O_2 at 37 °C. Intracellular Ca^{2+} concentration of DA SMCs was performed using the ARVO™MX fluorescence microplate reader (PerkinElmer Life Sciences) from 5 min at room air after the hypoxic incubation. Fura-2/AM was excited at 340 and 390 nm with fluorescence emission detected using a 510-nm band pass filter. We evaluated intracellular Ca^{2+} concentration with the use of the observed fluorescence ratio 340/390 nm.

Organ Culture—Ex vivo DA organ culture was prepared as described previously (21). Briefly, fetal arteries including the DA on the 19th day of gestation were stimulated for 2 days by *R*(−)-efonidipine under the following conditions: a humidified chamber, a concentration of 10^{-6} M in 0.5% FCS containing Dulbecco's modified Eagle's medium, 5% CO_2, and 95% ambient mixed air at 37 °C. The segments were fixed in 10% buffered formalin and embedded in paraffin. Morphometric analyses were conducted using Win Roof version 5.0 software (Mitani Corp., Tokyo, Japan). Intimal cushion formation was defined as [intimal area]/[medial area].

Isometric Tension of the DA Vascular Rings—After the maternal rats were anesthetized on the 21st day of gestation with an overdose of pentobarbital (100 mg/kg), the fetuses at embryonic day 21 were delivered by cesarean section. Either the vascular ring of the DA or the descending aorta was placed in a tissue bath and kept at 37 °C. Two tungsten wires (30 μm in diameter) were threaded into the lumen, and the preparation was mounted in a two-channel myograph (Dual Wire myograph system 410A; Unique Medical, Tokyo, Japan). One tungsten wire was connected to a micro-manipulator, and the other was connected to a force transducer. All of the vascular rings were initially stabilized for at least 60 min with a modified Krebs-Henseleit solution (Sigma-Aldrich) that was equilibrated with room air and whose temperature was maintained at 37 °C by a heated water jacket. Isometric tension was continuously monitored using a PowerLab/8 SP system (ADInstruments, Inc., Colorado Springs, CO). After stabilization, the vascular ring was exposed to 1 μM of indomethacin-containing Krebs-Henseleit solution for at least 10 min at 37 °C. After the vascular ring was washed with modified Krebs-Henseleit solution and relaxed, the resting tension was adjusted to 0.30 mN. After a plateau vasoconstriction had been attained using oxygen exposure (95% O_2, 5% CO_2), *R*(−)-efonidipine or the L-type Ca^{2+} channel blocker, nitrendipine, was added to stimulate vasodilatation. After the vasoconstriction reached a new steady state, the concentration of *R*(−)-efonidipine was increased from 10^{-7} M to 10^{-5} M. At the end of all experiments, vasoconstriction of the DA was induced by potassium-enriched solutions (22 mM NaCl, 120 mM KCl, 1.5 mM $CaCl_2$, 6 mM glucose, 1 mM $MgCl_2$, 5 mM HEPES, pH 7.4).

Time Course of DA Closure after Birth—After the maternal rats were anesthetized on the 21st day of gestation with an overdose of pentobarbital (100 mg/kg), rat newborns were obtained by cesarean section. Immediately after cesarean section, the neonates were given intraperitoneal injections either with *R*(−)-efonidipine at a concentration of 10 μg/g of body weight or 100 μg/g of body weight or with saline. After injection, the neonates were incubated in room air at 33 °C for 30 or 90 min, and then the DA segments were fixed and analyzed by the same method used in the organ culture. The degrees of vasoconstriction and intimal cushion formation were estimated by [open area]/[total vessel area] and [intimal area]/[medial area], respectively.

Statistical Analysis—All of the data are presented as the means ± S.E. Student's unpaired *t* tests were used to compare mRNA expression in the DA and other tissues. Comparisons between data from multiple groups were performed by unpaired analysis of variance followed by the Student's-Newmann-Keuls test. *p* values <0.05 were considered statistically significant.

RESULTS

α1G Protein Was Up-regulated and Localized in the Cells Sealing the Lumen of the DA after Birth—Our previous study demonstrated that α1G mRNA was predominantly expressed and were significantly up-regulated in the DA during vascular development (5). Then we examined the expression of α1G protein in the DA tissue during the perinatal period. Consistent with the change in the expression of mRNA, the expression levels of α1G protein were significantly up-regulated by 2.3-fold in the neonatal DA just after birth from what they were in the DA on embryonic day 21 (Fig. 1).

Because our previous study had demonstrated that α1G protein was strongly expressed in the region of intimal thickening of the mature DA at embryonic day 21 (5), we further investigated the localization of α1G protein in the DA after birth. We found that the lumen of the rat neonatal DA was filled with densely packed intimal cells within 1 h after birth, whereas the

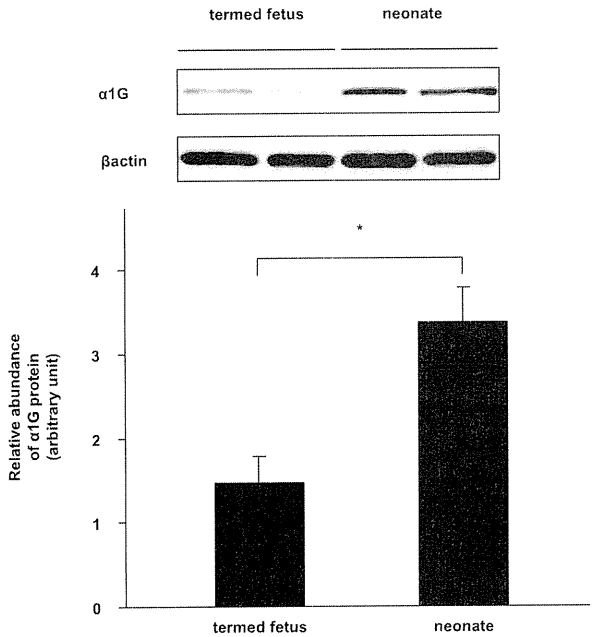

FIGURE 1. **Western blot analysis of the rat perinatal DA.** The expression levels of α1G protein were significantly up-regulated by 2.3-fold in the neonatal DA relative to that in the DA of termed fetuses. The values are expressed as the means ± S.E. ($n = 4$). * indicates $p < 0.01$.

lumen of the aorta was widely open (Fig. 2, *A* and *B*). The immunoreaction of α1G protein was strongly stained in these cells of the central core of the DA lumen (Fig. 2*C*). Ki-67, a nuclear antigen associated with cell proliferation, was also strongly stained in the packed intimal cells (Fig. 2*D*), suggesting that α1G is profoundly expressed in the proliferative cells.

Oxygenation Up-regulated the Expression of α1G in DA Smooth Muscle Cells—We then examined the effect of oxygenation on the expression of α1G in DA SMCs. When the condition of the culture medium was changed from hypoxia (1% oxygen) to normoxia (21% oxygen) in the DA SMCs after 7 h, the expression levels of α1G mRNA were up-regulated by 2.2-fold, and those of protein were up-regulated by 1.9-fold (Fig. 3), although they were unchanged after 1 h. These data may explain the association between the up-regulation of α1G in the rat neonatal DA and an increase in oxygen tension in the circulation after birth.

α1G Promoted SMC Migration of the DA—Progressive SMC migration from vascular media into the endothelial layer is an important vascular remodeling process of the DA at birth (1, 19, 23). These findings regarding the localization of α1G protein that was observed suggest that α1G regulated the SMC migration of the DA. First, when the expression of α1G mRNA was up-regulated by ~2.5-fold by transfection of α1G plasmids in DA SMCs (supplemental Fig. S2*A*), SMC migration was significantly increased by 2.1-fold ($p < 0.01$) (Fig. 4*A*). In the presence of 10% FCS, SMC migration was increased by more than 5-fold, probably because of hormones and/or cytokines that were contained in FCS. It should be noted that FCS did not significantly affect the expression of α1G mRNA (supplemental Fig. S3). α1G overexpression further increased FCS-mediated SMC migration by 1.6-fold ($p < 0.01$) (Fig. 4*A*). Next, we examined the effect of genetic and pharmacological inhibition of T-type VDCC on DA SMC migration. Two different siRNAs for α1G significantly decreased the expression of α1G mRNA and protein in DA SMCs by ~60% (supplemental Fig. S2, *B* and *C*), whereas they did not significantly change the expression of α1C, α1C splice variant, and α1D mRNAs that was abundantly detected in the rat DA (supplemental Fig. S4) After these α1G siRNAs were used, FCS-mediated SMC migration was significantly decreased by ~42% when compared with that of a nontargeting negative control siRNA (Fig. 4*B*). Furthermore, *R*(−)-efonidipine, a recently developed, highly selective T-type VDCC blocker, significantly attenuated FCS-mediated SMC migration by ~48% in a dose-

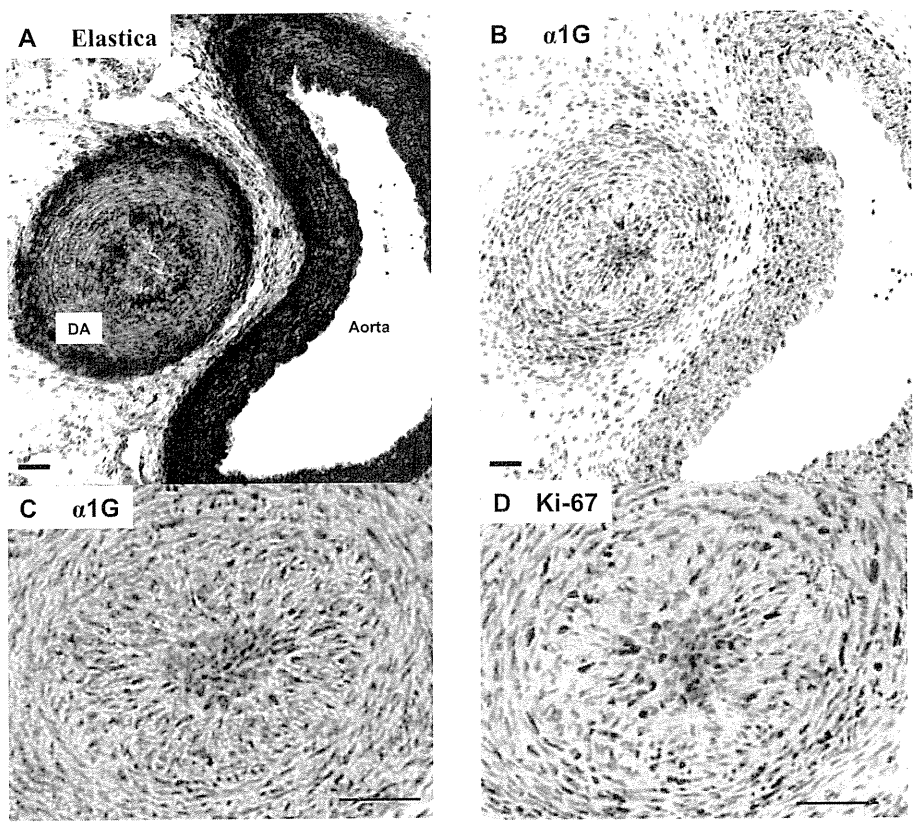

FIGURE 2. **Immunohistochemistry of rat neonatal DA.** *A*, elastica staining of the DA and the aorta. *B*, α1G subunit staining of the DA and the aorta. Strong immunoreaction was found in the DA. *C*, enlarged image of the DA stained by anti-α1G subunit antibody. *D*, Ki-67 staining. Strong immunoreaction was found in the overlapping region of the α1G subunit staining. *Scale bars*, 50 μm.

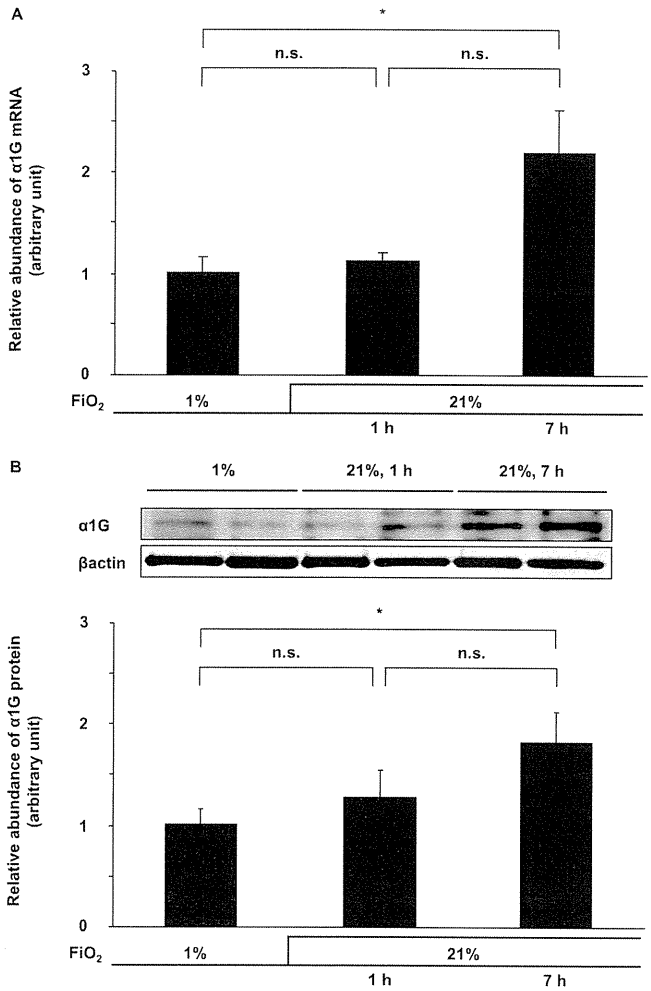

FIGURE 3. **Effects of oxygenation on α1G expression.** When the condition of the culture medium was changed from hypoxia (1% oxygen) to normoxia (21% oxygen), the expression levels of both α1G mRNA (*A*) and protein (*B*) were significantly up-regulated after 7 h by 2.2- and 1.9-fold, respectively. The values are expressed as the means ± S.E. ($n = 6$). * indicates $p < 0.01$. *n.s.*, not significant.

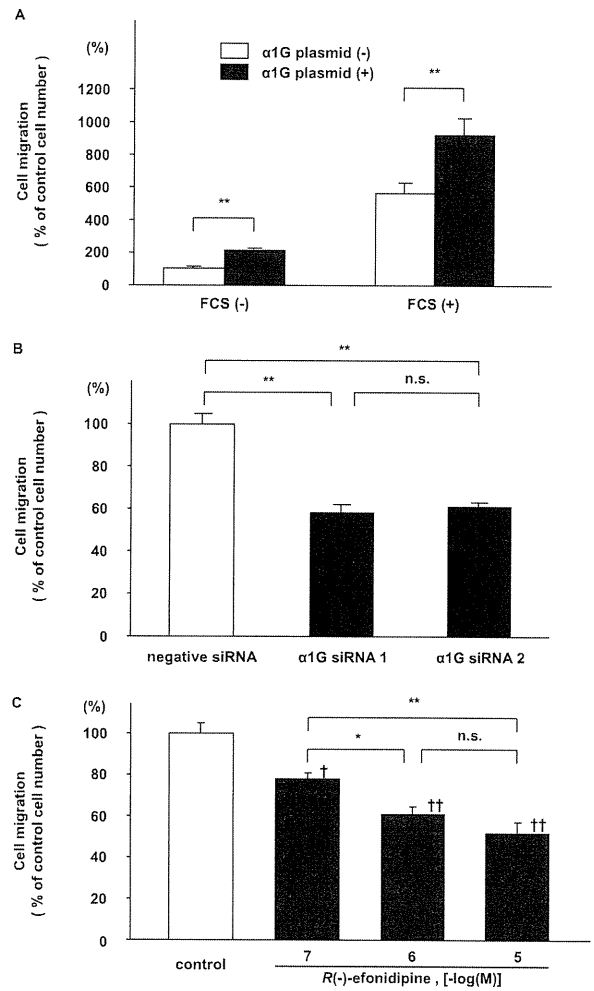

FIGURE 4. **DA SMC migration assay.** *A*, effects of α1G overexpression on DA SMC migration. Migration was significantly increased in α1G overexpressed SMCs when compared with that of control SMCs ($n = 7$). 10% FCS increased SMC migration by more than 5-fold. In the α1G-overexpressed cells, SMC migration was further increased by 1.6-fold ($n = 7$). *B*, effects of α1G-specific siRNAs on DA SMC migration. Two different α1G-specific siRNAs significantly decreased FCS-mediated SMC migration by ~58% when compared with a nontargeting negative control siRNA ($n = 11$). *C*, effects of *R*(−)-efonidipine on DA SMC migration. *R*(−)-efoidipine significantly attenuated DA SMC migration by ~52% in a dose-dependent manner ($n = 8$). The values are expressed as the means ± S.E. * and ** indicate $p < 0.05$ and $p < 0.01$, and † and †† indicate $p < 0.05$ and $p < 0.01$ *versus* control, respectively. *n.s.*, not significant.

dependent manner ($p < 0.01$) (Fig. 4*C*). Mibefradil, another selective T-type VDCC blocker, also significantly attenuated FCS-mediated SMC migration by ~17% in a dose-dependent manner ($p < 0.05$), although its inhibitory effect was weaker than that of *R*(−)-efonidipine (supplemental Fig. S5).

Oxygenation Was Required for α1G-mediated SMC Migration—Because vascular remodeling of the DA, including SMC migration, dramatically progresses after birth, we hypothesized that oxygenation might play a critical role in regulating this remodeling through an increase in Ca^{2+} influx via T-type VDCCs. When cultured DA SMCs were used and when the condition of culture medium was changed from hypoxia to normoxia, SMC migration was increased by ~2.0-fold in the normoxic group when compared with that in the hypoxic group, either in the absence or presence of 10% FCS ($p < 0.01$), indicating that oxygenation promoted SMC migration of the DA. Furthermore, we examined the effect of T-type VDCCs on oxygenation-mediated migration. We found that *R*(−)-efonidipine at a concentration of 10^{-6} M significantly attenuated DA SMC migration by ~23% when the culture medium was changed from hypoxia to normoxia ($p < 0.05$), although it exhibited no effect on SMC migration in a continuously hypoxic medium (Fig. 5*A*). In addition, using one of the α1G-specific siRNAs that significantly decreased the expression of α1G mRNA as presented above, we found that the α1G-specific siRNA significantly decreased DA SMC migration by ~42% when compared with a nontargeting negative control siRNA in a culture medium changed from hypoxia to normoxia ($p < 0.01$) (Fig. 5*B*). However, the α1G-specific siRNA did not suppress SMC migration in a continuously hypoxic medium. It should be noted that FCS was still capable of stimulating DA SMC migration even in the presence of *R*(−)-efonidipine and α1G-specific siRNA, suggesting that FCS contains some cell migrating fac-

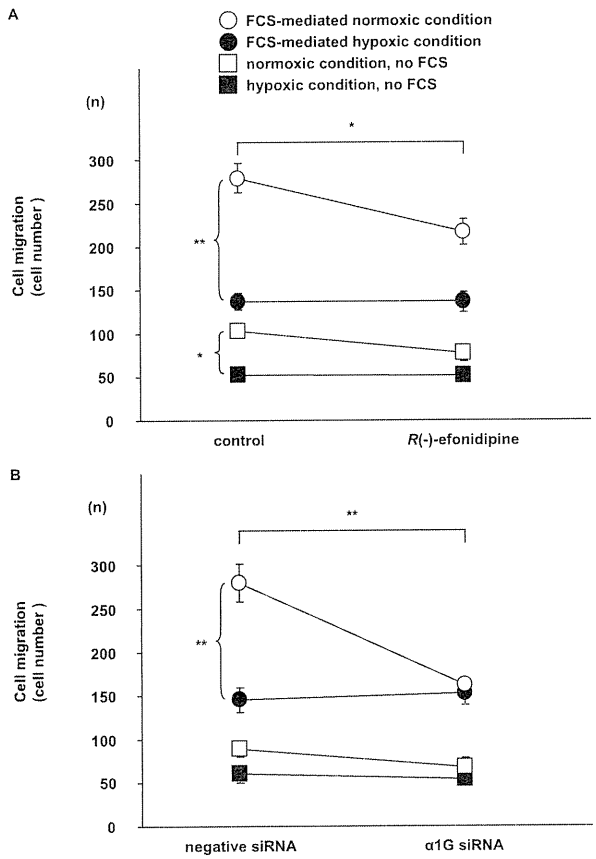

FIGURE 5. **Effects of oxygenation on DA SMC migration.** *A*, effects of *R*(−)-efoidipine on oxygenation-mediated DA SMC migration. *R*(−)-Efonidipine significantly attenuated DA SMC migration by ~77% in a culture medium changed from hypoxia to normoxia ($n = 8$). It should be noted that no effect of the α1G-specific siRNA and *R*(−)-efonidipine on SMC migration was observed in the hypoxic culture medium. *B*, effects of α1G-specific siRNA on oxygenation-mediated DA SMC migration. When the condition of the culture medium was changed from hypoxia to normoxia, SMC migration was significantly increased in the normoxic group when compared with that in the hypoxic group in the presence of 10% FCS ($n = 5$). DA SMC migration was significantly decreased by ~58% when compared with that of a nontargeting negative control siRNA in a culture medium changed from hypoxia to normoxia ($n = 5$). The values are expressed as the means ± S.E. * and ** indicate $p < 0.05$ and $p < 0.01$, respectively.

tors that are independent of the effect of T-type VDCCs on SMC migration. Taken together, these independent experiments indicated that T-type VDCCs, most likely α1G, played an important role in promoting oxygenation-mediated SMC migration in the DA.

α1G Regulated Oxygenation-induced Intracellular Ca^{2+} Increases—It has been known that oxygenation increases intracellular Ca^{2+} concentration of the DA to consequently initiate smooth muscle contraction of the DA (6, 24). Accordingly, using fura-2/AM fluorescence assay, we also found that intracellular Ca^{2+} concentration of cultured DA SMCs was significantly increased by ~1.3-fold by oxygenation when the condition of culture medium was changed from hypoxia to normoxia (Fig. 6, *A* and *B*). Importantly, we found that *R*(−)-efonidipine significantly inhibited the oxygenation-mediated increase in an intracellular Ca^{2+} concentration of cultured DA SMCs by ~12 or ~20% at a concentration of 10^{-7} or 10^{-6} M, respectively (Fig. 6, *C* and *D*). In addition, using one of the α1G-specific siRNAs that significantly decreased the expression of α1G mRNA as presented above, we found that the α1G-specific siRNA significantly decreased the oxygenation-mediated increase in intracellular Ca^{2+} concentration of cultured DA SMCs by ~15% (Fig. 6, *E* and *F*). Taken together, these data indicated that T-type VDCCs, most likely α1G, played an important role in the oxygenation-mediated increases in intracellular Ca^{2+} concentration of the DA.

R(−)-Efonidipine Inhibited EP4-mediated Intimal Thickening in the Rat DA—Our previous study had demonstrated that when immature rat DA explants were exposed to an EP4-specific agonist, ONO-AE1–329, for 48 h in an organ culture, intimal cushion formation was fully developed in DA explants (21). To investigate whether T-type VDCC indeed plays an important role in promoting intimal cushion formation, we examined the effect of *R*(−)-efonidipine on ONO-AE1–329-mediated intimal cushion formation in the rat DA explants (Fig. 7). The intimal thickening was 2.5-fold greater in the presence of ONO-AE1–329 than it was in the control (Fig. 7, *B* and *D*), which was consistent with our previous findings (21). *R*(−)-Efonidipine significantly inhibited ONO-AE1–329-mediated intimal cushion formation by 40% (Fig. 7, *C* and *D*). The immunostaining of Ki-67 of ONO-AE1–329-mediated intimal cushion formation was similar in the presence or absence of *R*(−)-efonidipine (supplemental Fig. S6).

R(−)-Efonidipine Attenuated Oxygenation-induced Vasoconstriction of the Rat DA—Because vasoconstriction is another important factor of DA closure, we examined the role of T-type VDCCs in DA vasoconstriction by exposing a vascular ring of the fetal DA at embryonic day 21 to oxygenating Krebs-Henseleit solution. *R*(−)-Efonidipine attenuated oxygenation-induced vasoconstriction in a dose-dependent manner (Fig. 8). Isometric tension induced by oxygen was attenuated by ~27% or by 40% in the presence of *R*(−)-efonidipine at a concentration of 10^{-6} or 10^{-5} M, respectively. *R*(−)-Efonidipine exhibits selective inhibition of T-type VDCCs at a concentration of 10^{-6} M, whereas it inhibits not only T-type but also L-type VDCCs at a concentration of 10^{-5} M (25). The data indicated that not only T-type but also L-type VDCCs contributed to oxygenation-induced vasoconstriction. In this regard, nitrendipine, a selective L-type VDCC blocker, additively inhibited oxygenation-induced vasoconstriction in the presence of *R*(−)-efonidipine (10^{-6} M) (data not shown).

R(−)-Efonidipine Delayed Closure of the Rat Neonatal DA—The present study demonstrated that Ca^{2+} influx via T-type VDCCs, especially α1G, stimulated SMC migration, intimal cushion formation, and vasoconstriction in the cultured DA SMCs or DA explants. It would be important to determine whether blockade of Ca^{2+} influx via T-type VDCCs indeed prevents *in vivo* DA closure after birth. To test this possibility, *R*(−)-efonidipine was intraperitoneally injected into rat newborns just after delivery by cesarean section. The data obtained is summarized in Table 1. All of the control DAs closed at 30 min after saline injection (Fig. 9*A*), whereas all of the DAs remained open at 90 min after ONO-AE1–329 injection (Fig. 9*D*). After injection of *R*(−)-efonidipine at a concentration of 10 μg/g of body weight, most (71%, five of seven neonatal rats) of the DAs remained open at 30 min,

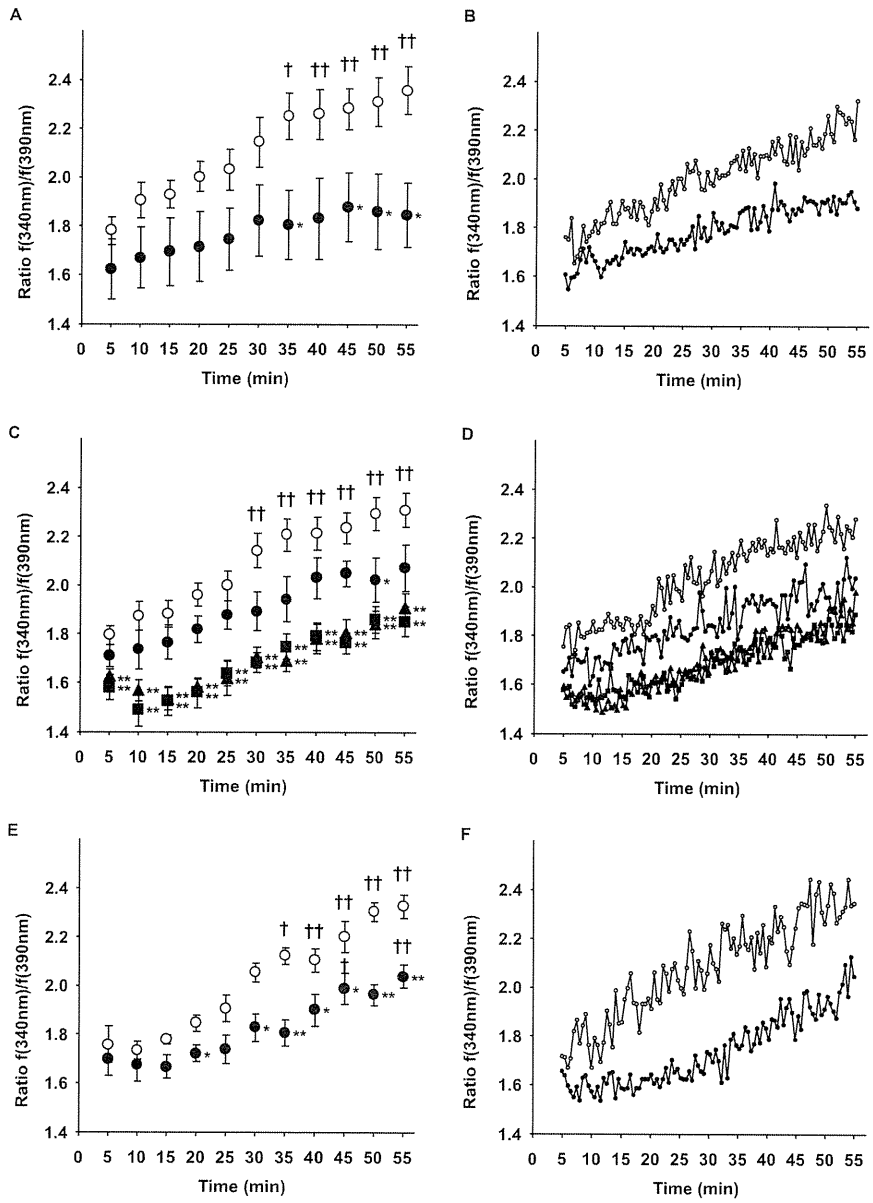

FIGURE 6. **Effects of oxygenation on intracellular Ca^{2+} concentration in DA SMCs.** *A*, effects of oxygenation on the fura-2/AM fluorescence ratio. When the condition of the culture medium was changed from hypoxia to normoxia, the fluorescence ratio 340/390 nm was significantly increased from 35 min after oxygenation (*open circle*, $n = 6$). The fluorescence ratio 340/390 nm was not significantly increased when the condition of the culture medium stayed in the normoxia (*closed circle*, $n = 6$). *B*, traces of the ratio of representative *A*. *C*, effects of *R*(−)-efonidipine on the oxygenation-mediated increase in the fura-2/AM fluorescence ratio. *R*(−)-Efonidipine at a concentration of 10^{-7} M significantly decreased the ratio by ~12% in only 50 min after oxygenation (*closed circle*, $n = 6$), when compared with controls (*open circle*, $n = 6$). *R*(−)-Efonidipine at a concentration of 10^{-6} M significantly decreased the ratio from 5 min after oxygenation, which decreased by ~20% (*closed triangle*, $n = 6$). *R*(−)-Efonidipine at a concentration of 10^{-5} M significantly decreased the ratio from 5 min after oxygenation, which decreased by at most 21% (*closed square*, $n = 6$). *D*, traces of the ratio of representative *C*. *E*, effects of α1G siRNA on oxygenation-mediated increase of the ratio. α1G siRNA significantly suppressed the oxygenation-mediated increases in the ratio by 15% from 20 min (*closed circle*, $n = 6$) when compared with a nontargeting negative control siRNA (*open circle*, $n = 6$). *F*, traces of the ratio of representative *E*. The values are expressed as the means ± S.E. † and †† indicate $p < 0.05$ and $p < 0.01$ *versus* 5 min after oxygenation, respectively, and * and ** indicate $p < 0.05$ and $p < 0.01$ *versus* the normoxic condition, respectively.

whereas less than half (43%, three of seven neonatal rats) remained open at 90 min (Fig. 9, *B* and *E*). Furthermore, when the dose of *R*(−)-efonidipine was increased to 100 μg/g of body weight, the percentage of patent DA was increased to 86% at both 30 and 90 min after injection of *R*(−)-efonidipine (Fig. 9, *C* and *F*). The ratio of [open area]/[total vessel area] was significantly increased by administration of *R*(−)-efonidipine ($n = 6$–7; Fig. 9*G*), suggesting that it attenuated vasoconstriction of the neonatal rat DA. The ratio of [intimal area]/[medial area] was significantly decreased by administration of *R*(−)-efonidipine ($n = 6$–7; Fig. 9*H*), suggesting that it inhibited intimal cushion formation. These data indicated that blockade of T-type VDCCs indeed delays closure of the rat neonatal DA through vasodilation and intimal cushion formation.

DISCUSSION

The present study revealed that T-type VDCCs, especially α1G subunit, play a role in promoting oxygenation-induced DA closure through vasoconstriction (functional closure) and intimal cushion formation (anatomical closure) in the rat neonatal DA. Accordingly, blockade of T-type VDCC using *R*(−)-efonidipine indeed retarded closure of the rat neonatal DA (Fig. 9 and Table 1).

In terms of functional DA closure, we found that blockade of T-type VDCC resulted in vasodilation of *ex vivo* rat DA (Fig. 8), using *R*(−)-efonidipine that exhibits more selective inhibition of T-type VDCC than that exhibited in other previous studies (6, 7). Although the effect of *R*(−)-efonidipine on vasorelaxation seemed relatively modest when compared with that on intracellular Ca^{2+} concentration, it should be noted that the protocols of the experiments were different for measurement of contractility and intracellular Ca^{2+} concentration. In the experiment for measurement of contractility, *R*(−)-efonidipine was added after oxygenation-induced vasoconstriction had already occurred. Because vasorelaxation is a relatively slow process, the inhibitory effect of *R*(−)-efonidipine on vasoconstriction seemed rather less than expected. In addition to T-type VDCC, other channels such as L-type VDCC and transient receptor potential channels are also involved in Ca^{2+} influx in the DA (6, 26) and should be taken into consideration.

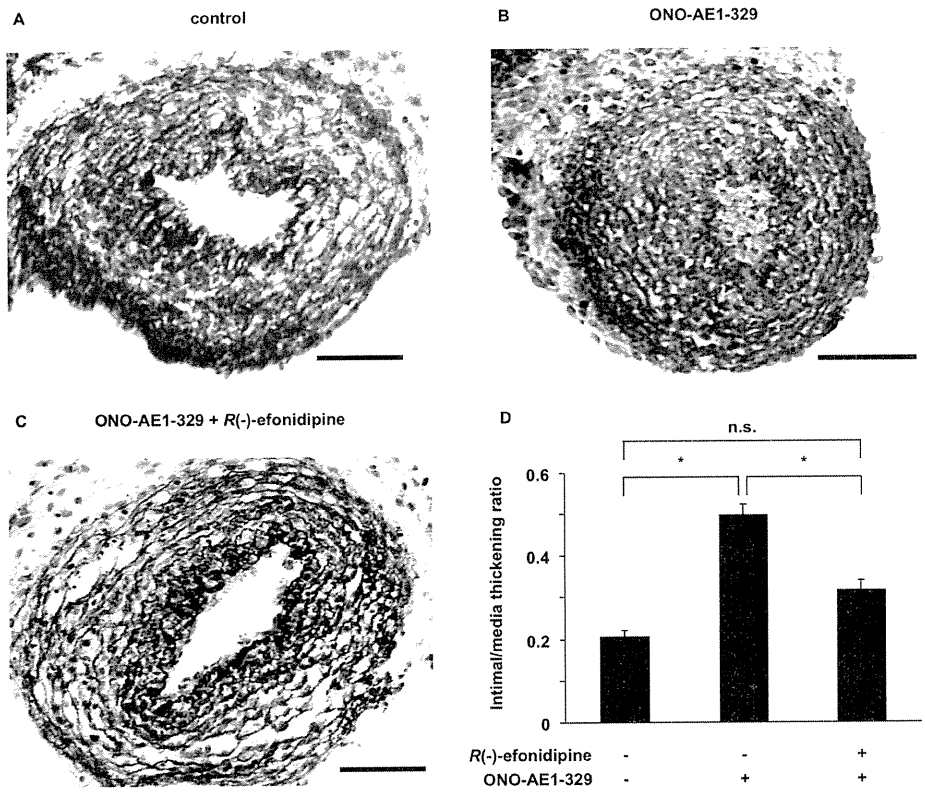

FIGURE 7. **Effects of R(−)-efonidipine on EP4-mediated intimal thickening of immature rat DA explants.** *A*, control. *B*, ONO-AE1–329 (10^{-6} M). *C*, ONO-AE1–329 (10^{-6} M) plus *R*(−)-efonidipine (10^{-6} M). *Scale bars*, 50 μm. *D*, the ratio of intimal and medial thickening. Intimal thickening was 2.5-fold greater in the presence of ONO-AE1–329 than it was in the control. *R*(−)-Efonidipine significantly inhibited ONO-AE1–329-mediated intimal cushion formation by 60%. The values are expressed as the means ± S.E. ($n = 5$). * indicates $p < 0.01$. *n.s.*, not significant.

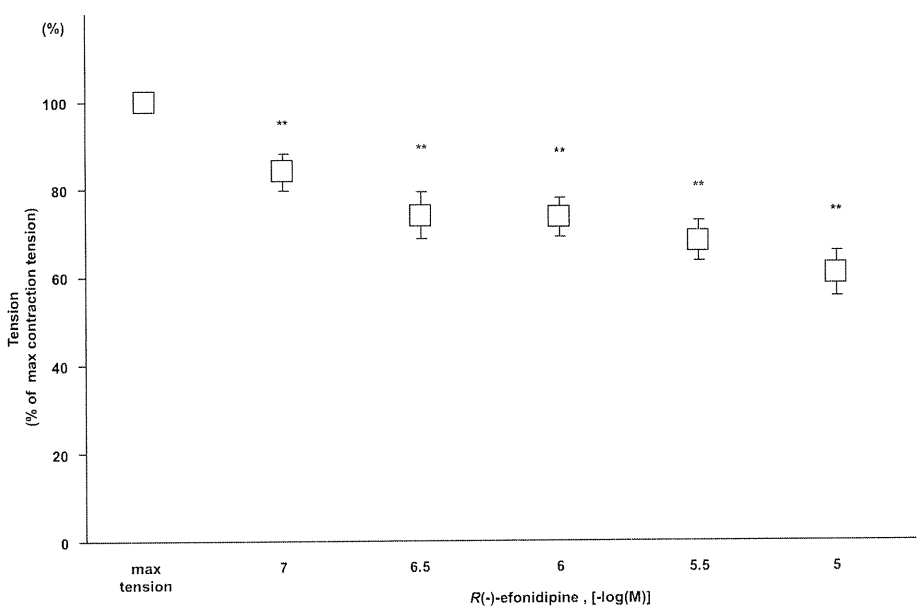

FIGURE 8. **Effects of R(−)-efonidipine on vasoconstriction of rat DA.** DA tension as a function of *R*(−)-efonidipine. *R*(−)-Efonidipine significantly attenuated oxygen-induced vasoconstriction in a dose-dependent manner ($n = 18$). The values are expressed as the means ± S.E. ** indicates $p < 0.01$ *versus* maximal vasoconstriction.

In terms of anatomical DA closure, we found that *R*(−)-efonidipine inhibited intimal cushion formation in the rat DA explants. Schmitt *et al.* (27) have demonstrated that blockade of T-type VDCC using mibefradil prevents pathological neointimal formation after vascular injury. Although the mechanism has not been well understood, several studies, including our previous one, have indicated that T-type VDCC promotes both proliferation (5, 18, 28) and migration of vascular SMCs (16). However, T-type VDCC may not significantly increase cell proliferation and thus EP4-mediated intimal cushion formation, because *R*(−)-efonidipine did not affect the expression of Ki-67 in the DA explants in the presence of ONO-AE1–329 (supplemental Fig. S6) Therefore, SMC migration must be involved in T-type VDCC-mediated intimal cushion formation. Accordingly, using both molecular and pharmacological approaches in our present study, we found that Ca^{2+} influx through T-type VDCC promotes SMC migration when cells were harvested in a normoxic condition and that DA SMC migration is promoted in accordance with an increase in extracellular Ca^{2+} concentration (supplemental Fig. S7). It should be noted that several studies have demonstrated that L-type VDCC also promotes SMC migration and thus neointima formation in other vessels (14, 17, 29), although the findings are more controversial than those on T-type VDCC. In our unpublished experiments, we found that nitrendipine, a selective L-type VDCC blocker, also inhibits FCS-mediated SMC migration in the rat DA. A further study warrants examination of which type of Ca^{2+} channels plays a more significant role in neointima formation of the DA.

Interestingly, the effect of T-type VDCC on SMC migration was not observed in the hypoxic condition of the culture medium (Fig. 5). Importantly, oxygenation increased intracellular Ca^{2+} concentration that was significantly inhibited by *R*(−)-efonidipine (Fig. 6). These results suggested that oxygenation activates T-type VDCC, increases intracellular Ca^{2+} concentration, and then promotes migration of DA SMCs. In this sense, several studies have demonstrated that reactive oxygen species

TABLE 1

Patent DA ratio and DA patency ratio when two different substances were intraperitoneally injected into rat newborns at two different times just after delivery by cesarean section

Substance injected (dosage)	Time after injection	DA patency ratio[a]
	min	%
Saline	30	0/6 (0)
R(−)-Efonidipine (10 μg/g of body weight)	30	5/7 (71)
R(−)-Efonidipine (100 μg/g of body weight)	30	6/7 (86)
Saline	90	0/6 (0)
R(−)-Efonidipine (10 μg/g of body weight)	90	3/7 (43)
R(−)-Efonidipine (100 μg/g of body weight)	90	6/7 (86)
ONO-AE1–329 (10 ng/g of body weight)	90	3/3 (100)

[a] Number of experiments in which DA patency was observed per number of experiments. The numbers in parentheses indicate the percentages of patent DA.

enhance the activity of T-type VDCC (30) and that hypoxia inhibits the activity (31). Furthermore, we found that oxygenation up-regulated the expression levels of α1G subunit in DA SMCs. Consistently, the expression levels of α1G subunit protein in the DA were significantly up-regulated after birth, which happens to be when oxygen tension in circulatory blood is dramatically increased. Although several studies have demonstrated that hypoxia up-regulated the expression of T-type VDCCs (32, 33), to our knowledge, our report is the first one showing that oxygenation up-regulated the expression of α1G mRNA and protein. Because oxygenation is known to promote DA closure after birth, the present data highlight another important role of oxygenation in the vascular remodeling through T-type VDCC. We, however, could not define the mechanism by which oxygenation activates T-type VDCC and up-regulates the expression of α1G in the present study. This important question should be addressed in our future study.

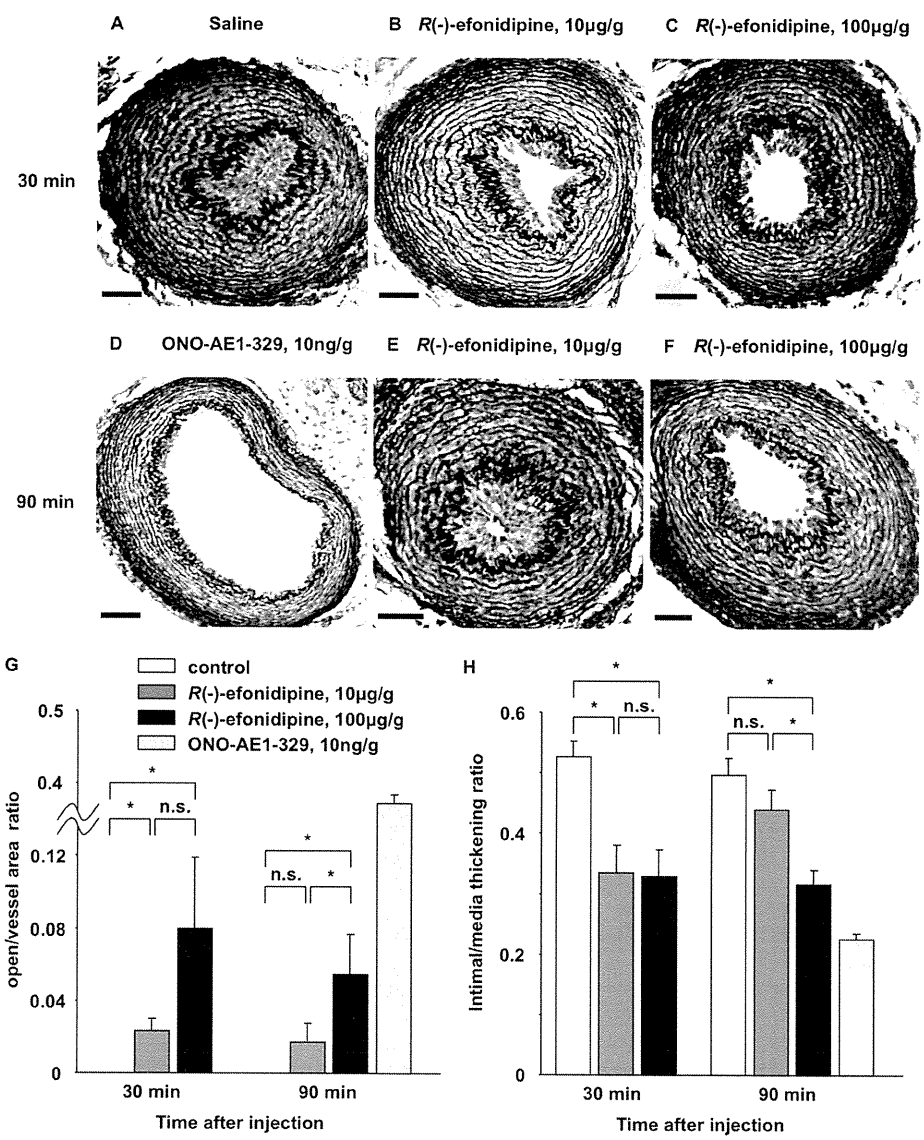

FIGURE 9. **Effects of R(−)-efonidipine on the patency of *in vivo* rat neonatal DA.** *A–F*, representative morphology of the neonatal DA 30 min after peritoneal injection of saline (*A*), of *R*(−)-efonidipine (10 μg/g of body weight) (*B*), and of *R*(−)-efonidipine (100 μg/g of body weight) (*C*), and 90 min after injection of ONO-AE1–329 (10 ng/g of body weight) (*D*), of *R*(−)-efonidipine (10 μg/g of body weight) (*E*), and of *R*(−)-efonidipine (100 μg/g of body weight) (*F*). *Scale bars*, 50 μm. *G*, the ratio of [open area]/[total vessel area] *versus* time after injection. The ratio was significantly increased by administration of *R*(−)-efonidipine. *H*, the ratio of [intimal area]/[medial area] *versus* time after injection. The ratio was significantly decreased by administration of *R*(−)-efonidipine. The values are expressed as the means ± S.E. ($n = 6–7$). * indicates $p < 0.05$. *n.s.*, not significant.

Although T-type VDCC is not the only factor (channel) in DA closure, T-type VDCC, especially α1G, plays a unique role in DA closure for the following reasons: 1) the expression of α1G is highly restricted in the DA, especially after birth, whereas that of other Ca^{2+} channels may not be, and 2) T-type VDCC promotes both functional and anatomical closure of the DA. These characters of α1G T-type VDCC are important, particularly for clinical applications. For example, blockade of T-type VDCC does not have serious adverse effects such as hypotension or cardiac dysfunction (34), whereas blockade of L-type VDCC may induce hypotension or cardiac dysfunction (35), especially in neonates. These adverse events are critical to keep the DA open in patients with congenital heart diseases involving right- or left-sided obstruction, because their circulatory systems are usually less compliant. For these patients, prostaglandin E_1 administration is commonly used as the most potent vasodilator of the DA (1). However, our previous study supports the notion that chronic prostaglandin E_1 stimulation may have an adverse effect on such patients because it also promotes anatomical DA closure. On the contrary, blockade of T-type VDCC prevents both vasoconstriction and EP4-mediated intimal cushion formation of the DA.